

NASA SUPPORT

IN-07

56633
787.

DOT/FAA/CT-86/10

FAA TECHNICAL CENTER
Atlantic City Airport
N.J. 08405

Quantitative Determination of Engine Water Ingestion

(NASA-CR-180188) QUANTITATIVE DETERMINATION
OF ENGINE WATER INGESTION Final Report, May
1984 - Dec. 1985 (Jet Propulsion Lab.) 78 p

CSCL 21E

N87-17702

Unclass

G3/07 43338

P. Parikh
M. Hernan
V. Sarohia

Jet Propulsion Laboratory
California Institute of Technology
Pasadena, California 91109

December 1986

Final Report

This document is available to the U.S. public
through the National Technical Information
Service, Springfield, Virginia 22161.



U.S. Department of Transportation
Federal Aviation Administration

NOTICE

This document is disseminated under the sponsorship of the Department of Transportation in the interest of information exchange. The United States Government assumes no liability for the contents or use thereof.

The United States Government does not endorse products or manufacturers. Trade or manufacturer's names appear herein solely because they are considered essential to the object of this report.

Technical Report Documentation Page

1. Report No. DOT/FAA/CT-86/10	2. Government Accession No.	3. Recipient's Catalog No.	
4. Title and Subtitle QUANTITATIVE DETERMINATION OF ENGINE WATER INGESTION		5. Report Date December 1986	
7. Author(s) P. Parikh, M. Hernan and V. Sarohia		6. Performing Organization Code	
9. Performing Organization Name and Address Jet Propulsion Laboratory California Institute of Technology 4800 Oak Grove Drive Pasadena, CA 91109		8. Performing Organization Report No. JPL Publication No. D-3041	
12. Sponsoring Agency Name and Address U.S. Department of Transportation Federal Aviation Administration Technical Center Atlantic City Airport, New Jersey 08405		10. Work Unit No. (TRAIS) 11. Contract or Grant No. DTFA03-81-A-00765	
		13. Type of Report and Period Covered Phase I May 84-Dec. 85	
15. Supplementary Notes Project Manager, Tom Rust, Engine/Fuel Safety Branch, Aircraft and Airport Safety Technology Division, FAA Technical Center		14. Sponsoring Agency Code	
16. Abstract This report describes a non-intrusive optical technique for determination of liquid mass flux in a droplet laden airstream. The technique was developed for quantitative determination of engine water ingestion resulting from heavy rain or wheel spray. Independent measurements of the liquid water content (LWC) of the droplet laden airstream and of the droplet velocities were made at the simulated nacelle inlet plane for the liquid mass flux determination. The liquid water content was measured by illuminating and photographing the droplets contained within a thin slice of the flow field by means of a sheet of light from a pulsed laser. A fluorescent dye introduced in the water enhanced the droplet image definition. The droplet velocities were determined from double exposed photographs of the moving droplet field. The technique was initially applied to a steady spray generated in a wind tunnel. It was found that although the spray was initially steady, the aerodynamic breakup process was inherently unsteady. This resulted in a wide variation of the instantaneous liquid water content of the droplet laden airstream. The standard deviation of ten separate LWC measurements was 31 percent of the average. However, the liquid mass flux calculated from the average LWC and droplet velocities came within 10 percent of the known water ingestion rate.			
17. Key Words Engine water ingestion wheel spray Two phase flow measurement	18. Distribution Statement This document is available to U.S. Public through the National Technical Information Service, Springfield, Virginia 22161		
19. Security Classif. (of this report) Unclassified	20. Security Classif. (of this page) Unclassified	21. No. of Pages	22. Price

ACKNOWLEDGEMENTS

This work was sponsored at the Jet Propulsion Laboratory of California Institute of Technology by the U.S. Department of Transportation, Federal Aviation Administration Technical Center through NASA Contract NAS7-918, agreement No. DTFA03-81-A-00765. The authors extend their gratitude to Messrs. T. Rust, F. Howard, and W. T. Westfield of FAA Technical Center for their guidance and suggestions. The assistance of Messrs. W. Bixler and S. Kikkert in fabrication of the apparatus is gratefully acknowledged.

PRECEDING PAGE BLANK NOT FILMED

TABLE OF CONTENTS

	PAGE
EXECUTIVE SUMMARY	viii
INTRODUCTION	1
REVIEW OF APPLICABLE MEASUREMENT TECHNIQUES	1
PRESENT TECHNIQUE	2
WATER INGESTION SIMULATION FACILITY	8
IMAGE PROCESSING SYSTEM DESCRIPTION	10
RESULTS AND DISCUSSION	13
CONCLUDING REMARKS	17
REFERENCES	19
APPENDICES	
A. Image Analysis Program	A-1
B. Droplet Statistics Program	B-1
C. Droplet Data	C-1
D. Distribution List	D-1

PRECEDING PAGE BLANK NOT FILMED

LIST OF ILLUSTRATIONS

FIGURE		PAGE
1	Droplet Illumination and Photographic System	4
2	Droplet Photograph Without Fluorescent Dye in the Water	5
3	Droplet Photograph With Fluorescent Dye in the Water	6
4	Double Pulse Photograph of Droplets in a Moving Air Stream	7
5	Schematic Diagram of Engine Water Ingestion Simulation Facility	9
6	Typical Photograph of the Droplet Field at the Nacelle Inlet Plane	11
7	Image Processing System Architecture	12
8	Digital Subimage Representing One Grid Square	14
9	Enhanced Version of Digital Subimage Shown in Figure 9	14
10	Droplet Size Distribution at the Nacelle Inlet Plane	18

NOMENCLATURE

A_f Frontal area of nacelle. (m^2)
D Droplet Diameter (mm)
LWC Liquid Water Content (gm/m^3)
 \dot{m}_w Mass flow rate of water (gm/sec)
n Number of drops counted
q_w Total liquid volume in the measurement volume (cm^3)
Q_w Volumetric water ingestion rate (cm^3/sec)
V_a Airspeed (m/sec)
V_w Water jet speed at the spray nozzle (m/sec)
V_d Average water drop speed (m/sec)
x distance downstream from the spray nozzle (m)

Greek Letters

ρ_w Water density (gm/cm^3); 1.0 gm/cm^3
 δ Thickness of the Light Sheet (mm)

Subscripts

a Average spray property
i Identify i^{th} drop, where $i = 1$ to n

EXECUTIVE SUMMARY

Water droplet ingestion into turbine engines resulting from heavy rain and wheel spray generated on a wet runway is of importance. Adverse effects of large quantities of water ingestion can include the compressor stall and combustor flame-out. Engine certification requirements as set forth in FAA regulations call for continued engine operation at takeoff and flight idle conditions while ingesting water at 4 percent by weight of airflow, generated by a spray to simulate rain. There is also a certification requirement on the entire aircraft system which dictates that the system must be designed to prevent hazardous quantities of water from being ingested into the engine during takeoff, landing and taxiing operations on wet runways. The present work was undertaken to develop measurement techniques of two-phase droplet laden airstreams during engine water ingestion. The ultimate objective is to correlate the non-intrusive measurements of the water ingestion rate and droplet size and spatial distribution at the engine inlet with engine performance parameters. Such techniques and data will assist the FAA in evaluating current water ingestion certification tests.

A non-intrusive optical technique was developed for the determination of liquid mass flux in a droplet laden airstream. The technique is also capable of providing information on the droplet size and spatial distribution at the nacelle inlet plane.

Independent measurements of the liquid water content (LWC) of the droplet laden airstream and of the droplet velocities were made at the inlet plane of a simulated nacelle in a wind tunnel for the liquid mass flux determination. The liquid water content was determined by illuminating and photographing the droplets contained within a thin slice of the flow-field by means of a sheet of light from a pulsed laser. Fluorescent dye introduced in the water enhanced the droplet image definition. The droplet velocities were determined from double exposed photographs of the moving droplet field. The technique was initially applied to a steady spray generated in a wind tunnel. It was found that although the spray was initially steady, the aerodynamic breakup process was inherently unsteady. This resulted in a wide variation of the instantaneous liquid water content of the droplet laden airstream. The standard deviation of ten separate LWC measurements was 31 percent of the average. However, the liquid mass flux calculated from the average LWC and droplet velocities came within 10 percent of the known water ingestion rate.

INTRODUCTION

The effects of water droplet ingestion into turbine engines resulting from heavy rain and wheel spray generated on a wet runway is of importance. The effects of water ingestion on engine performance have recently been investigated (reference 1) and a probe for stagnation pressure measurement in a droplet laden airflow was developed (reference 2). The adverse effects of large quantities of water ingestion can include the compressor stall and combustor flame-out (reference 1). Engine certification requirement as set forth in FAA regulations (reference 3) call for continued engine operation at takeoff and flight idle conditions while ingesting water at 4 percent by weight of airflow, generated by a spray to simulate rain. There is also a certification requirement on the entire aircraft system which dictates that the system must be designed to prevent hazardous quantities of water from being ingested into the engine during takeoff, landing, and taxiing operations, (reference 4).

The criteria for both water ingestion certification tests are somewhat arbitrary. The 4 percent by weight water ingestion test for engine certification does not address such issues as droplet size and their spatial distribution over the frontal area of the nacelle. For performance on a wet runway, the criterion is even more arbitrary in that it does not specify what constitutes a hazardous quantity of water ingestion.

The present work was undertaken to develop measurement techniques in two-phase droplet laden airstreams to better quantify the engine water ingestion. The ultimate objective is to correlate non-intrusive measurements of the water ingestion rate and droplet size and spatial distribution at the engine inlet with engine performance parameters. Such techniques and data will assist the FAA in evaluating current water ingestion certification tests.

REVIEW OF APPLICABLE MEASUREMENT TECHNIQUES

A review of available measurement techniques for sprays was undertaken to determine the applicability of the existing techniques to quantitative determination of water ingestion into an engine. The quantities that need to be determined are:

- a) Drop size distribution together with spatial distribution of drops at the nacelle inlet.
- b) The mass flow rate of water crossing the nacelle inlet plane at any instant.

Extensive work on measurements of wheel sprays generated by aircraft under-carriages was carried out by Barrett (reference 5). A spray intensity probe was developed to measure mean local dynamic pressure generated by moving droplets. However, all of Barrett's measurements were in the near field of the wheel generating the spray and the technique used only provided time averaged local measurements in the spray.

Several mechanical, electrical, and optical methods are available for droplet size determination in fuel sprays as surveyed in review articles by Jones

(reference 6) and, McCreathe and Beer (reference 7). None of the techniques surveyed would be capable, in their existing form, of satisfying the second requirement above. It was considered possible that the requirement could be met by some modification of the existing techniques.

The first trial approach was an extension of the charged wire probe technique described by Gardiner (reference 8) for drop size determination in water sprays. In that technique, the electrical pulse generated in a circuit containing a charged electrode when a drop impacts the electrode is measured by a pulse height analyzer. The probe is initially calibrated using known size drops impacting the electrode. A relationship is established between the pulse height and the drop size. In practice, the drop size characteristics are derived from the pulse height statistics stored in a pulse height analyzer. The technique as described by Gardiner (reference 8) thus provides the local drop size distribution in a spray. In the present work, a modification of the technique was considered. Instead of a single electrode probe, a charged grid was considered. A copper wire mesh with wire spacing of approximately 1 mm was charged to 2000 volts by a high voltage DC power supply. The idea was to install the screen at the nacelle inlet plane so that all drops larger than the mesh size would be intercepted by the screen. The charge transfer between the screen and the impacting drops would set up a current in the circuit supplying the grid. The current would be proportional to the total surface area of the drops impacting per unit time. Then if the size distribution were to be determined by an independent optical technique, the volume flow rate of water would be proportional to the product of the Sauter Mean Diameter (SMD) of the spray and the current supplied to the grid.

In practice, however, several difficulties were encountered with this technique.

- 1) The charge distribution on the screen was non-uniform, resulting in different pulse characteristics for different impact locations on the screen for the same size drop.
- 2) Wetting of the screen altered the initial charge distribution.
- 3) Water film on the support set up a conduction path from the screen to the ground, causing a leakage current.

Because of these difficulties and the fact that an optical technique was still needed in conjunction with the charged screen for water flow determination, this approach was abandoned in favor of a purely optical non-intrusive technique.

PRESENT TECHNIQUE

A non-intrusive optical technique was developed for the determination of drop sizes, spatial distribution of drops at the nacelle inlet plane and instantaneous mass flow rate of liquid water entering the nacelle. The liquid water mass flow rate is determined by independent measurements of the liquid water content of the droplet laden airstream and the droplet velocity at the nacelle inlet plane.

For liquid water content (LWC) determination, a thin cross-section of the flow close to the nacelle inlet plane is illuminated by a pulsed laser light sheet. The drops contained within this light sheet are photographed by a camera placed with its axis nearly normal to the plane of the light sheet (figure 1). The duration of illumination of drops by the laser pulse is extremely short, about 10 nano second. Therefore, the motion of the drops is frozen in the photographs. The thickness of the laser sheet is controlled by a beam expander and a slit. The slit was of 9 mm width while the initial beam width was 14 mm. The slit thus allowed only the intense central portion of the expanded beam to pass through, cutting off the less intense outer portions.

The depth of field of the camera is set to be larger than the light sheet thickness by proper selection of aperture and magnification. This assures that all illuminated drops (contained within the light sheet) appear in the photographs with a sharp edge definition. The measurement volume is defined by the product of the projected frontal area of the nacelle and the light sheet thickness. Information on drop sizes and spatial distribution is also obtained from this photograph.

When drops are photographed using the optical set up as shown in figure 1, with proper focusing and depth of field selection, the droplet edge definitions in the resulting photographic images are still far from ideal as shown in figure 2. This is caused by two effects:

- 1) The illumination of individual drops is not uniform, resulting in poor image definition of larger drops.
- 2) Scattering and diffraction around smaller drops causes a "halo" effect around the drop boundary, causing the image to appear much larger than the actual size.

An improved version of this technique utilizes laser induced fluorescence of a small quantity (less than 10 ppm) of dye (Rhodamine 6G or Fluorescene) introduced in the water. The fluorescence spectrum of the dye lies in a wavelength range longer than that of the incident light, therefore, the incident light scattered from the drops can be filtered out and only the fluoresced light is photographed. Shott colored glass filters are ideally suited for this purpose. This technique results in much better edge definition of droplets in the photographic images and a nearly uniform illumination of droplet interior (see figure 3).

An automated digital image processing system was developed to analyze the photographic images. The image processing algorithm detected drop edges, defined droplet boundaries, calculated the area of the drop images and an equivalent drop diameter based on this area. Droplet size distributions were constructed once statistics on a sufficient number of drops were available. The liquid water content was determined from the total volume of drops contained within the projected area of the nacelle, together with the knowledge of the incident light sheet thickness. A description of the image processing system is presented later in this report.

For the determination of instantaneous mass flow rate of airborne liquid water, a measurement of drop velocities is needed in addition to the LWC measurement. This may be accomplished non-intrusively by laser double pulse photography of the moving droplet field. Two images of each drop appear in the photograph (see figure 4) and the drop velocity may be determined by the measurement of

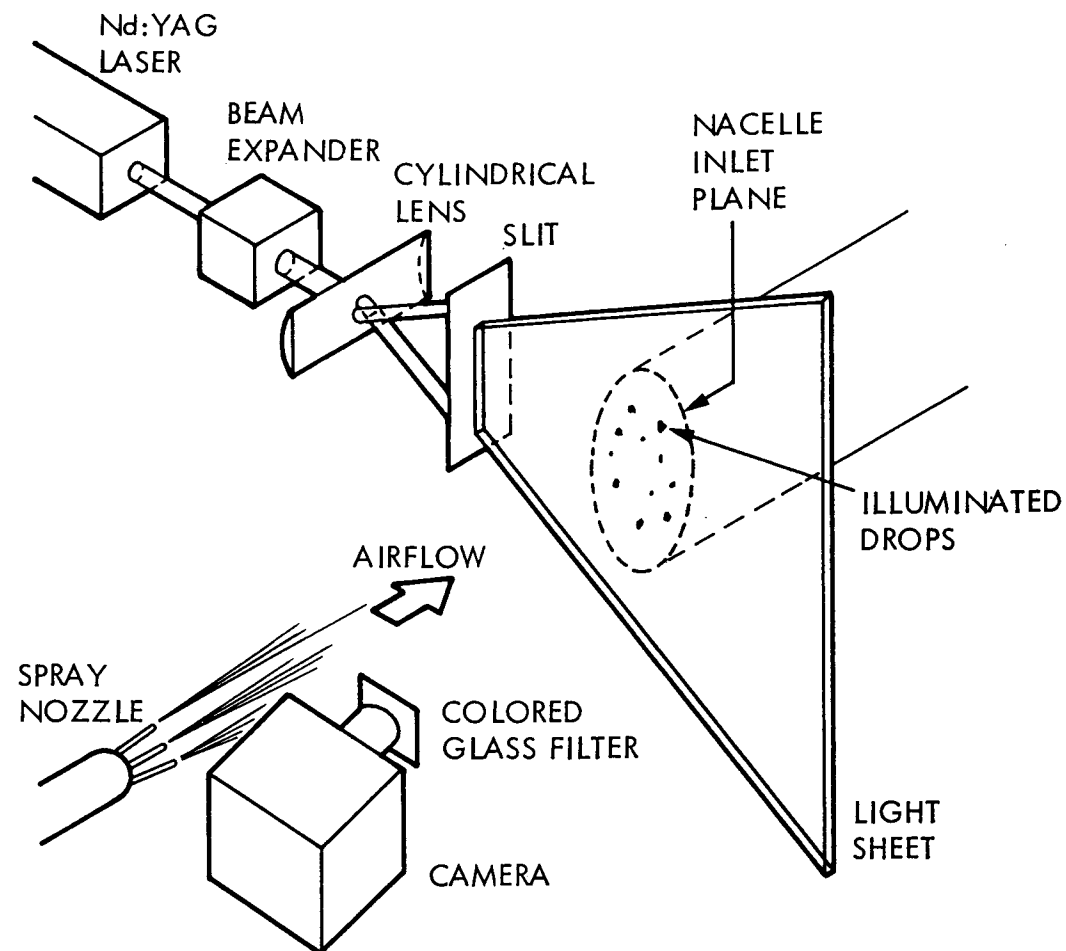


Figure 1. Droplet Illumination and Photographic System

ORIGINAL PAGE IS
OF POOR QUALITY

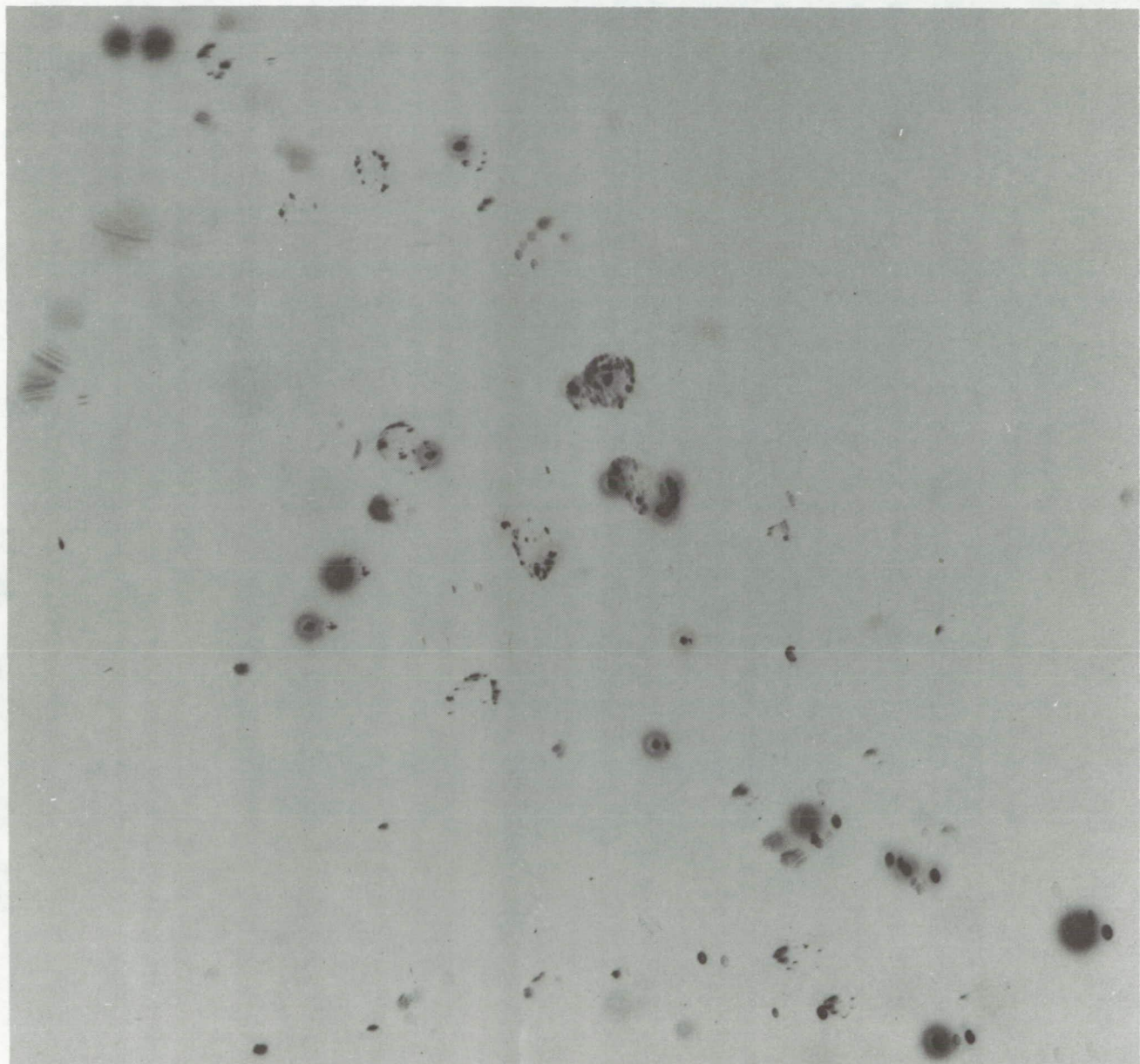


Figure 2 . Droplet Photograph Without Fluorescent Dye in the Water

ORIGINAL PAGE IS
OF POOR QUALITY

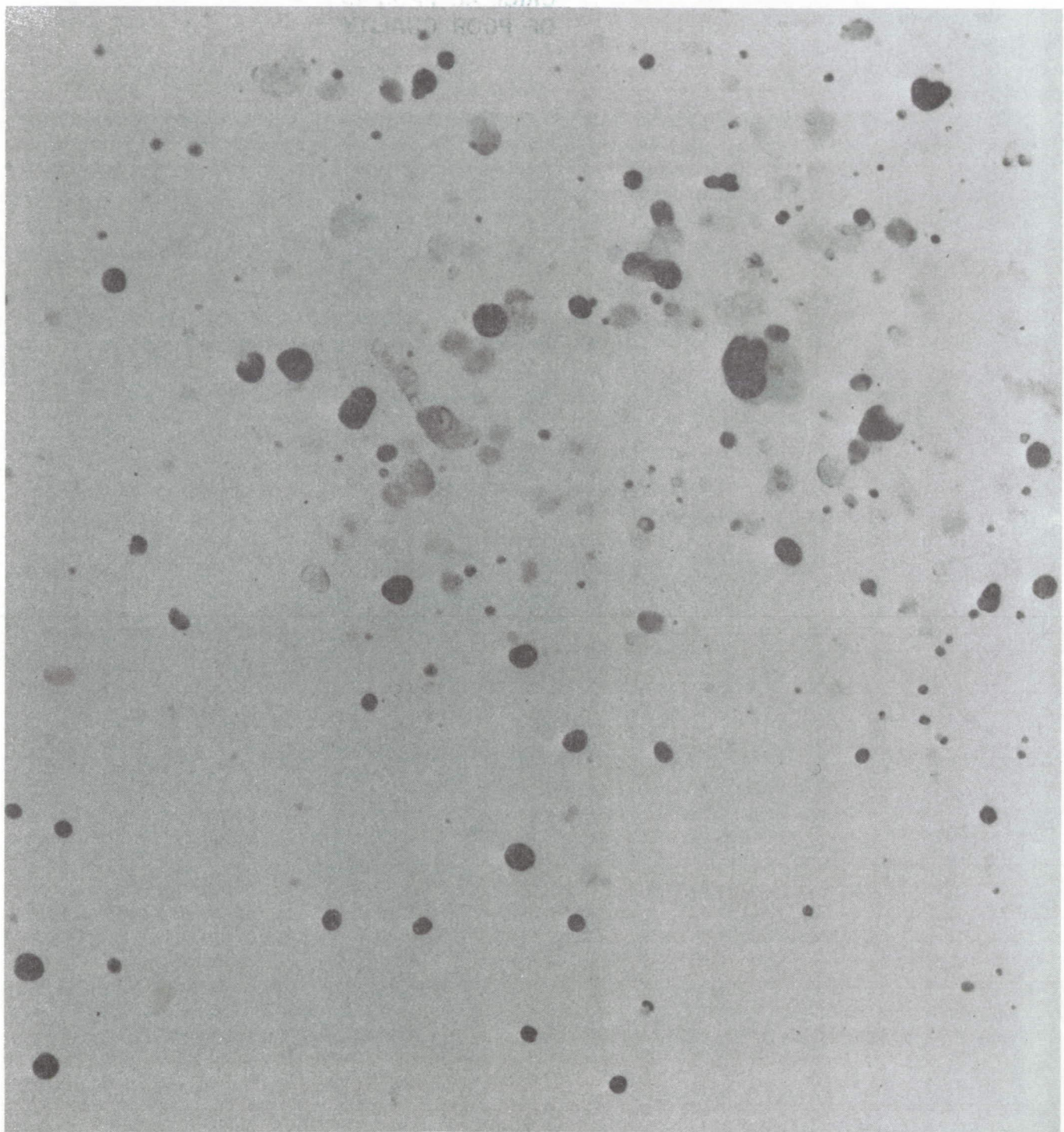


Figure 3. Droplet Photograph With Fluorescent Dye in the Water

ORIGINAL PAGE IS
OF POOR QUALITY

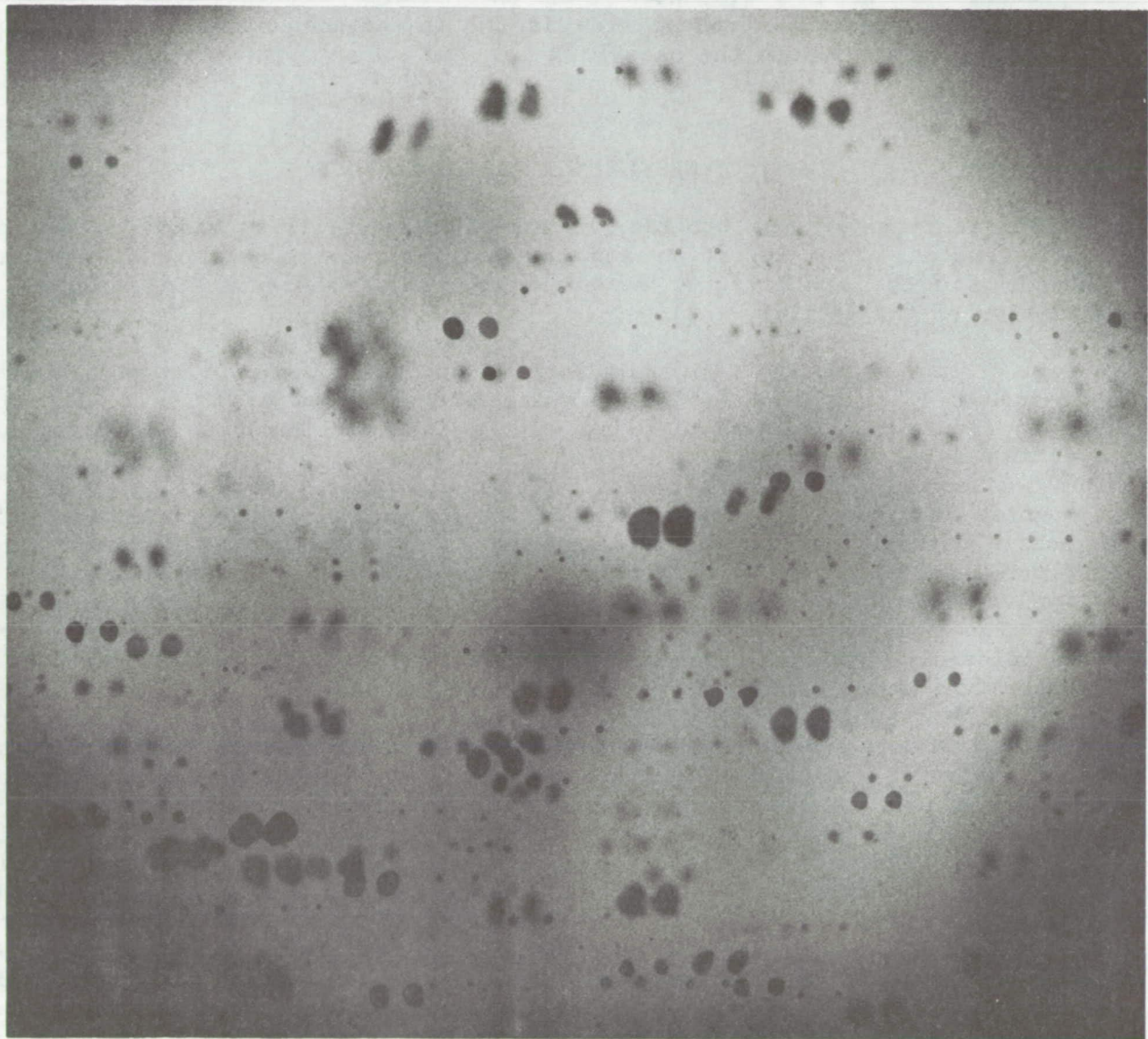


Figure 4. Double Pulse Photograph of Droplets in a Moving Air Stream

the distance translated in a known time interval. Solid-state lasers such as Ruby or Neodymium: yttrium aluminum garnet (Nd:YAG) lasers may be operated in the double pulse mode, wherein the Q-switch is opened twice in rapid succession to split the energy of the flash tube between two intense pulses. The time interval between the two pulses may be adjusted in the range of 50 to 200 μ s.

The product of the LWC evaluated over the nacelle frontal area, the drop velocity and the nacelle frontal area is the instantaneous mass flow rate of airborne liquid water into the nacelle.

WATER INGESTION SIMULATION FACILITY

In the first phase of the program, an experimental facility was developed to simulate engine water ingestion and to calibrate the non-intrusive optical technique for the quantitative measurements of engine water ingestion. A description of the facility follows.

The engine water ingestion simulation was set up in an open circuit wind tunnel of 18-inch x 18-inch test section. A schematic diagram of this facility is shown in figure 5. Air was supplied to the test section by a high capacity blower via a settling chamber, screens and a nozzle contraction. The blower output was adjusted by a damper vane ring at the inlet. A water spray nozzle was mounted on a streamlined sting support at the entrance to the test section. The nozzle consisted of seven 2 cm long tubes of 1.6 mm inside diameter. The water was supplied to the nozzle from a pressurized tank via a flowmeter and a ball valve. The individual tubes of the spray nozzle were adjusted such that most of the spray water entered the simulated nacelle with the tunnel running. The droplet-air mixture entering the simulated nacelle passed through a separator box which contained a series of baffle plates. The baffle plates subjected the flow to a series of sharp turns, thereby separating the droplets from the airstream and collecting them in a water film on the plate surfaces. Most of the water entering the nacelle in the form of droplets was collected at the bottom of the separator box. The air was evacuated from the separator box by means of the suction provided by the inlet of a secondary blower. The air from the exit side of the secondary blower was dumped back into the tunnel, downstream of the nacelle location. Calibration checks were made to determine the carry over loss of water in the form of fine drops. For the spray flow rate employed (300 cc/sec), the carry over loss was about 5 percent, with 95 percent of the water sprayed into the nacelle being collected at the bottom of the separator. With a steady spray, the total mass of water collected, divided by the time of collection was close to the time averaged mass flow rate of water entering the nacelle in the droplet-air mixture.

The optical set up is shown in figure 1. The laser sheet of 9 mm thickness was produced in front of the nacelle inlet plane approximately 2 mm from the inlet plane to avoid illuminating the water film on the rounded nacelle entrance. The illuminated droplet field was viewed through the side of the tunnel. The camera axis formed an angle of approximately 20 degrees with the nacelle axis. In viewing the droplet field through the plexiglas wall of the tunnel at such a shallow angle, multiple reflections of illuminated drops were encountered within the plexiglas wall. To alleviate this problem, a window extension was mounted on the tunnel side wall at a 20 degree angle, such that the camera line of sight was normal to the window at the end of the extension.

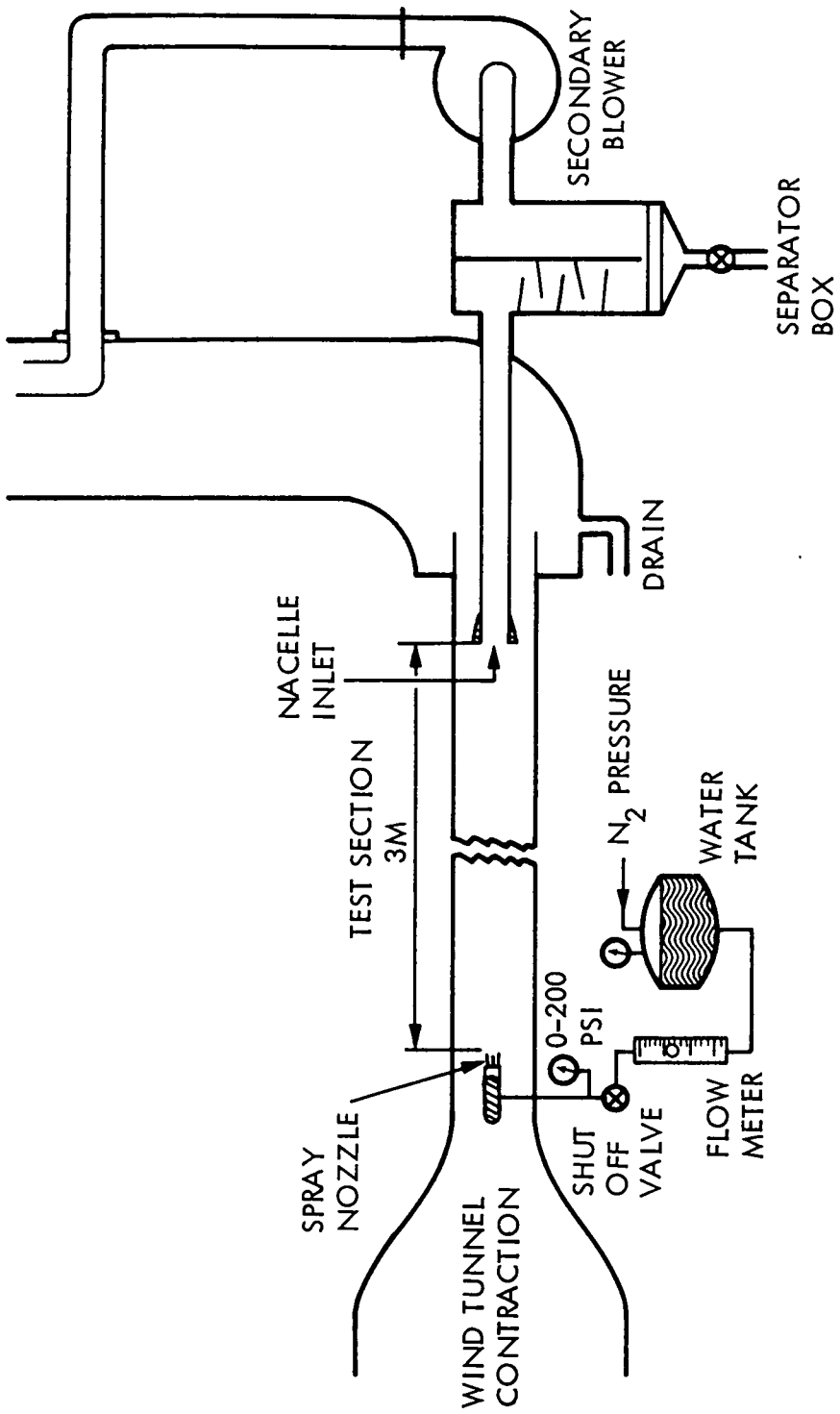


Figure 5. Schematic Diagram of Engine Water Ingestion Simulation Facility

The objective of the experiments was to compare the instantaneous water flow rate into the nacelle as determined by the present non-intrusive optical technique with the known time averaged water flow rate. Ten photographs were taken for a fixed spray rate and airspeed to yield a set of ten successive LWC measurements in a steady spray. The variation in the drop velocities within a given double exposed photograph or between two photographs at fixed tunnel speed and water injection pressure was found to be less than 5 percent. Therefore, a single drop velocity was used for water mass flow rate determination. A sample photograph of droplet field is shown in figure 6. The nacelle boundary was photographed separately and superimposed onto the droplet photograph in figure 6. Notice that the drops within the light sheet are uniformly illuminated and appear with sharp boundaries. Unfortunately, due to light scattered from drops contained in the light sheet and that from the beam dump and the transmitting side plexiglas window, some of the drops outside the laser sheet appear with faint images. During image processing of the photographic negatives, these faint drops, which are present outside the light sheet may easily be eliminated by setting proper threshold criteria.

IMAGE PROCESSING SYSTEM DESCRIPTION

Processing system architecture is depicted in figure 7. Image acquisition, display and processing was accomplished using a De-Anza ID-5400 image processing system. The hardware package incorporates a vidicon and power supply for analog image formation, three image refresh random access memory channels, RAM, digital video array processor, and color video display. The analogue signal from the video camera can be digitized by an A/D converter and fed directly to the array processor which in turn controls the data flow and writes the data into one of the memory planes at a rate of 30 frames/sec. The digitization process converts each picture into 512*512 matrix element (pixels). Each pixel is one byte number (256 resolution level) representing the average optical density in an elementary cell, the size of which dictates the spatial resolution of the system. While digitization can proceed at video rates of 30 frames per second, a program is used which creates one digital frame from the average of 64 consecutive digitized frames. Thus, the image formed has a low level of random noise caused by the vidicon and the digitizer electronics. The digitized image information is then stored on a mass-storage device for further off-line processing.

Software residing in the host computer (PDP 11/34) operates through a direct memory access (DMA), interface through which the PDP-11 sends and receives information from the video processor registers or from the RAM channels via a driver program. The vidicon image digitization, averaging and storage capability is part of this (DMA) interface software.

To study a droplet picture, the negative is taped on to a transparency containing a 1 cm x 1 cm grid formed by fine lines. The grid lines are carefully oriented with respect to the droplet images on the negative such that none of the drop images is intersected by the grid lines. The negative, together with the grid lines, is then mounted on a flat light-table. The vidicon is focused on the plane of the background illuminated negative by means of a macro lens. The magnification on to the vidicon is adjusted such that a 1 cm^2 area of the negative enclosed by the superposed grid lines nearly fills a video frame containing the 512 x 512 pixel array. After accounting for the photographic magnification of the image on the negative and a specification of

ORIGINAL PAGE IS
OF POOR QUALITY

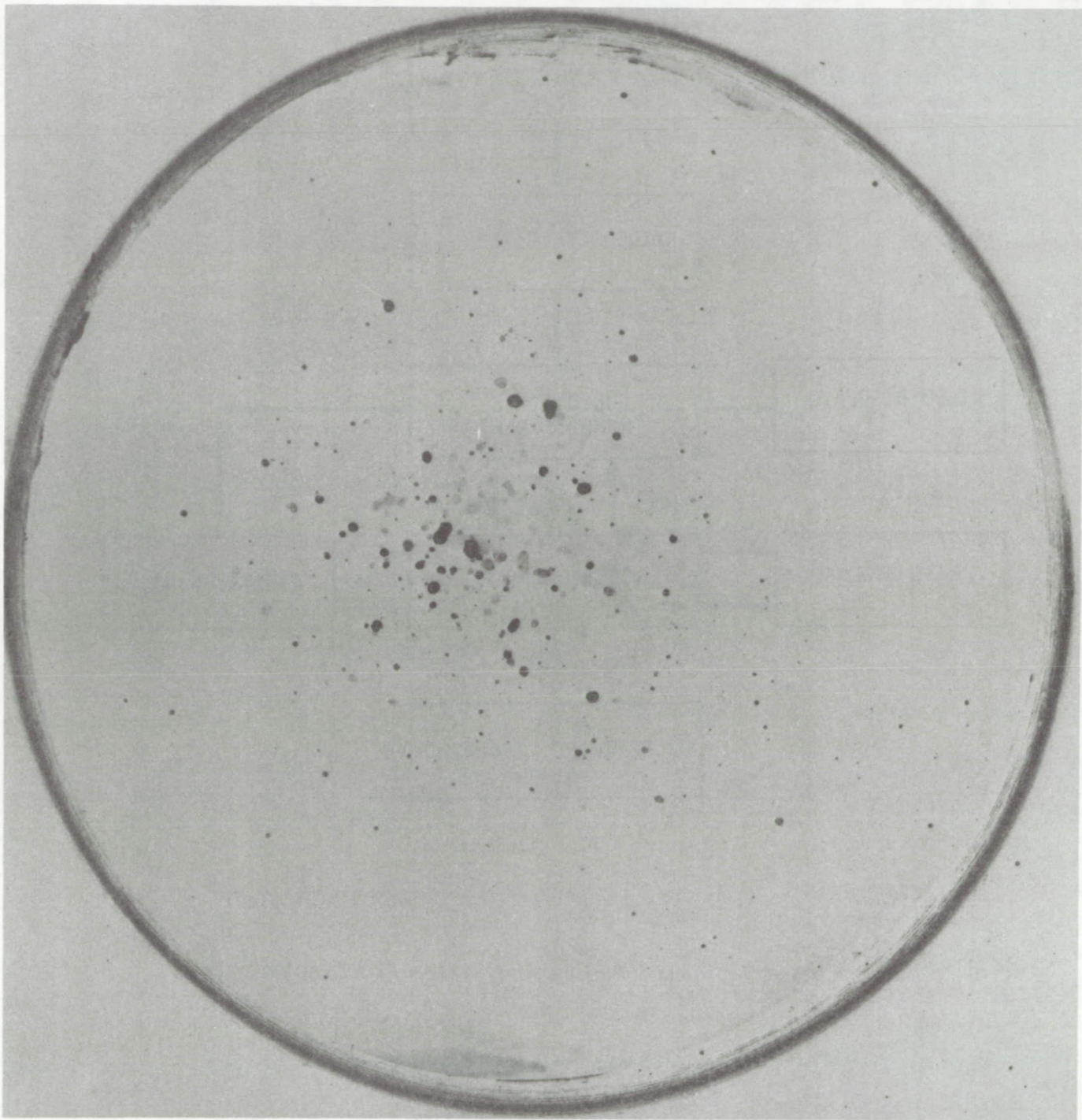


Figure 6. Typical Photograph of the Droplet Field at the Nacelle inlet plane

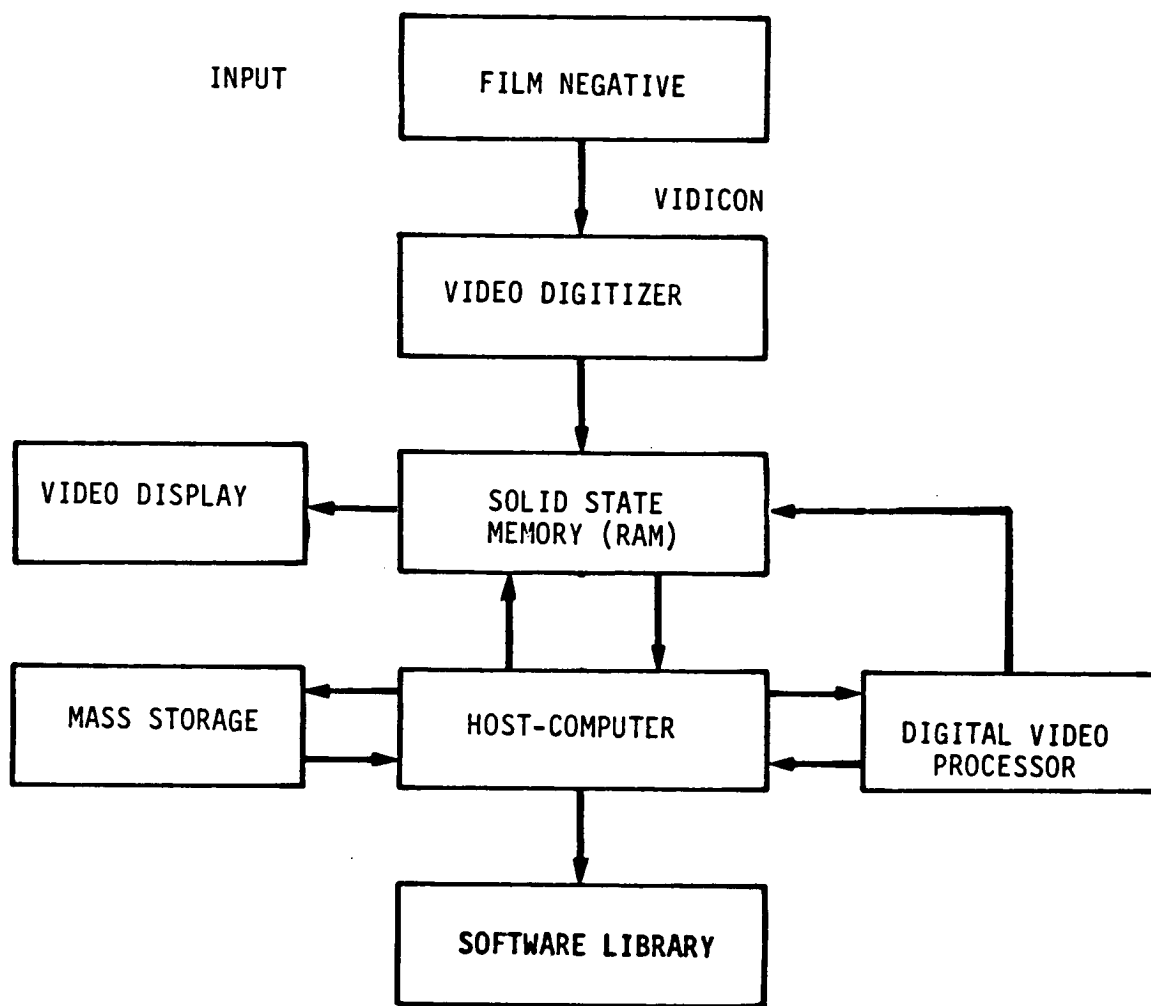


Figure 7. Image Processing System Architecture

4 pixels for the minimum size drop accepted, an overall resolution of 0.1 mm was estimated for the diameter of the smallest drop measured.

The negative was scanned, one grid square at a time over the projected frontal area of the nacelle. The calculated drop volumes were then added up for all the squares to evaluate the liquid water content over the projected frontal area of the nacelle. This procedure ensured that every drop is accounted for and is counted only once. An example of a digital subimage representing one grid square is shown in figure 8. An enhanced image with defined droplet boundaries is shown in figure 9.

Image processing software was developed to detect drop edges, define droplet boundaries, and calculate the area of drop images. The excellent contrast between the images of drops within the light sheet and the background allowed a simple thresholding criterion to define regions containing drop images.

The various image processing programs along with computer program needed for droplet statistics determination are attached under Appendices A and B, respectively.

RESULTS AND DISCUSSION

Results are presented here for fixed values of spray flow rate and airspeed in the wheel spray simulation tunnel. The flow rate through the spray nozzle was maintained constant at 0.3 liters/sec, which resulted in a water jet velocity of 22 m/s based on the total flow area of the seven tubes in the spray nozzle. As discussed later, this flow rate was chosen to simulate extreme cases of engine water ingestion resulting from wheel spray. The airspeed was maintained at 61 m/s. The large difference between the speeds of the air and the water jets caused an aerodynamic breakup of the water jets into small drops, which accelerated along the flow direction to approach the airspeed. The measurement station was located 3 m downstream of the spray nozzle and immediately upstream of the simulated nacelle inlet.

The droplet velocities were determined from a double exposed photograph of the moving droplet field as shown in figure 4. A 100 μ s time interval between the two pulses was employed. The droplet velocities were found to be within 5 percent for a large number of droplet pairs. Furthermore, within this small variation of droplet velocities, no correlation was found between the drop velocity and size. A single average value of velocity was assigned to all droplets. This average value was found to be only 41 m/s, i.e., 67 percent of the airspeed. Thus, the 3 m distance between the spray nozzle and the measurement station was insufficient to accelerate the drops to the tunnel airspeed.

A series of ten photographs was taken during the period January-February 1986 for the liquid water content determination. The width of the light sheet was maintained at 9 mm. The photographic negatives were analyzed by the image processing technique discussed in this report. The volume of a drop was calculated as the volume of a spherical drop having the same equivalent diameter. The equivalent diameter was calculated from the image area of each drop. For a non-spherical drop this procedure leads to a higher value of the calculated drop volume. The percentage error introduced therefore depends upon the how different the drop is as compared to the spherical shape.

ORIGINAL PAGE IS
OF POOR QUALITY

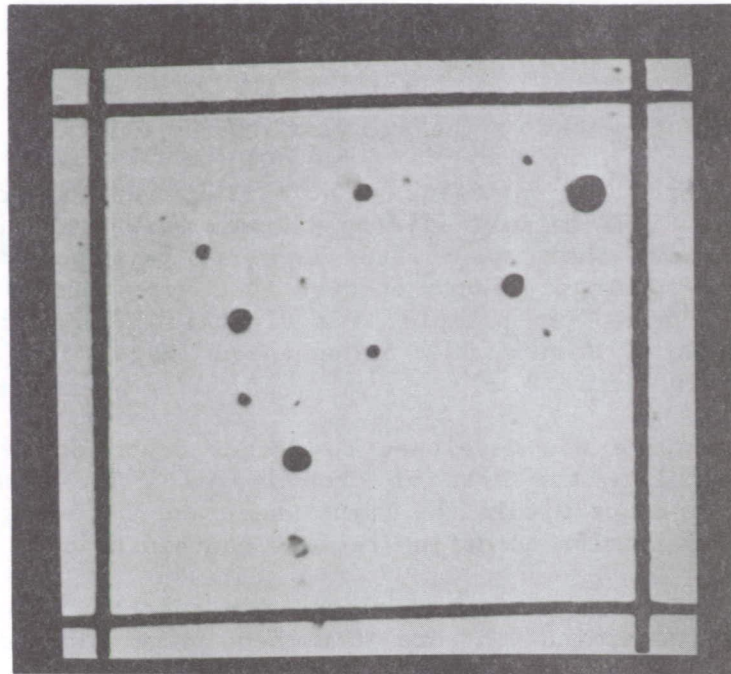


Figure 8. Digital Subimage Representing One Grid Square

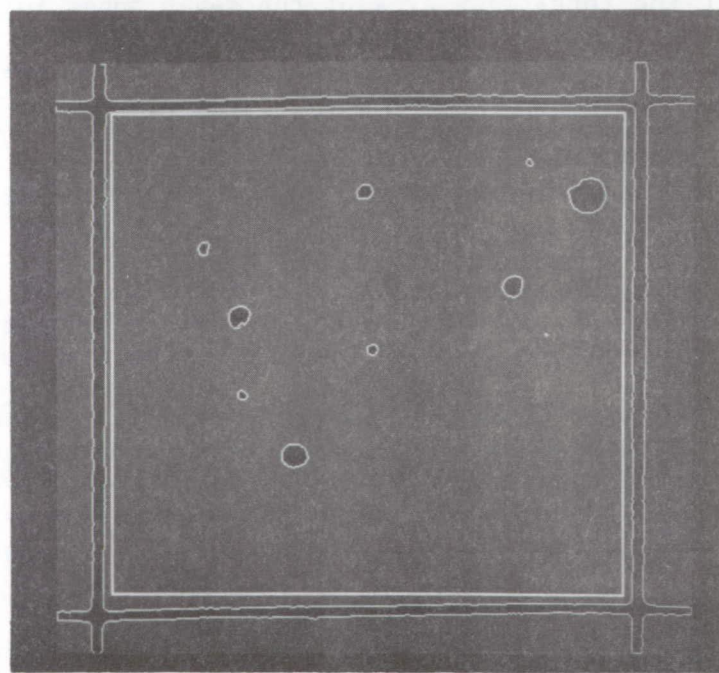


Figure 9. Enhanced Version of Digital Subimage Shown in Figure 8

The results of the image processing analysis are shown in table I. The raw droplet data has been shown under Appendix C. For each of the ten droplet pictures analyzed, the total number of drops counted over the nacelle frontal area, the mean droplet diameter, the volume weighted mean diameter and the total liquid volume are presented. The standard deviation of the mean and volume weighted mean droplet diameters as calculated from the ten pictures was in the range of 7 to 8 percent of the average. This indicated that the picture-to-picture variation of the calculated mean diameter was relatively small. The picture-to-picture variation of the total liquid volume was larger: the standard deviation of the ten measurements was 31 percent of the average. The average value of the total liquid volume from the ten pictures was used to calculate the average liquid water content, i.e.,

$$(LWC)_a = \frac{\rho_w q_w}{A_f \cdot \delta} = 450 \text{ gm/m}^3; \text{ where } \rho_w = 1.0 \text{ gm/cm}^3$$

The average mass flow rate of water was then calculated as

$$\begin{aligned} \dot{m}_w &= (LWC)_a \cdot A_f \cdot V_d \\ &= 332.5 \text{ gm/sec} \end{aligned}$$

The average mass flow rate of water in the moving droplet-air mixture as measured by the present non-intrusive optical technique thus indicates a flow rate approximately 10 percent higher than the actual value of 0.3 l/s. Reasons for this discrepancy between the measured and the actual mass flow rates are discussed below. It should be noted however, that there is a significant picture-to-picture variation in the instantaneous water mass flow rate determinations caused by measured variations in the instantaneous LWC values. The test droplet spray was quite dense in comparison with the certification requirement of 4 percent by weight of liquid water in the airstream. The present 0.3 l/s water ingestion rate in a 61 m/s airstream over the frontal area of the 15.24 cm diameter nacelle translates to a water flow rate/airflow rate ratio of 22.5 percent. Such a high water spray rate was used to simulate extreme cases of engine water ingestion resulting from wheel spray.

There are three factors that affect the accuracy of LWC measurement by the present technique:

- 1) Droplets largely outside the light sheet but at the boundary are partially grazed by the light sheet and show up on photographs, thus increasing the LWC measured.
- 2) The procedure for calculation of drop volume from its non-spherical images on the photograph relies on an equivalent diameter which is calculated from the enclosed area of the image. This procedure tends to over-predict the volume of the non-spherical drop and hence leads to a higher value of measured LWC.
- 3) The illuminated drops contained in the light sheet are viewed by the camera through a dense spray. Therefore, there is a possibility of some illuminated drops being masked by droplets present in the view path of the camera. This masking will result in a lower value of the measured LWC.

TABLE I
Summary of Data Photographs

$V_a = 61 \text{ m/s}$; $V_w = 21.7 \text{ m/s}$; $Q_w = 300 \text{ cm}^3/\text{sec}$; $x = 3 \text{ m}$; $A_f = 182.4 \text{ cm}^2$;
 $\delta = 9 \text{ mm}$

Negative No.	No. of Drops -	Mean Dia. mm	Vol. Mean Dia. mm	Total Liquid Vol. mm ³
1	267	0.55	0.89	97.4
2	207	0.58	0.86	68.2
3	256	0.51	0.87	89.0
4	155	0.58	0.86	52.3
5	179	0.63	0.92	88.0
6	212	0.56	0.88	75.0
7	243	0.59	0.91	95.7
8	128	0.50	0.68	21.5
9	337	0.53	0.80	91.8
10	169	0.60	0.87	57.8
Average:		0.56	0.85	73.7
Standard Deviation:		0.04	0.066	23.0
Std Dev. percent of Mean:		7.0	7.8	31.0

NOTE: Mean Dia. = $\frac{\sum n_i D_i}{\sum n_i}$; Vol. Mean Dia. = $\frac{\sum n_i D_i^4}{\sum n_i D_i^3}$

Total Liquid Vol. = $\sum n_i \frac{\pi}{6} D_i^3$

Despite these three sources of errors, the present non-intrusive technique is still considered a good method for measurement of the liquid water flow rate in a moving droplet-laden airstream.

The droplet size distribution determined from the more than 2000 drops counted in the ten pictures is shown in figure 10.

CONCLUDING REMARKS

- 1) A non-intrusive optical technique has been developed for quantitative determination of instantaneous liquid water mass flow rate in a droplet laden airstream. The technique is generally applicable to the problem of water ingestion into an engine resulting in up to 22% water by weight (rain or wheel spray).
- 2) The technique yields instantaneous spatial distribution of droplets at the nacelle inlet plane as well as the droplet size distribution.
- 3) Significant variation in the instantaneous values of the liquid water content was encountered in a droplet laden airstream produced by injection of a steady water spray in a steady airstream. The standard deviation among ten separate instantaneous determinations of the LWC was 31 percent of the average LWC.
- 4) The average liquid water flow rate as determined from the average LWC and drop velocity measurements was approximately 10 percent higher than the actual spray flow rate.

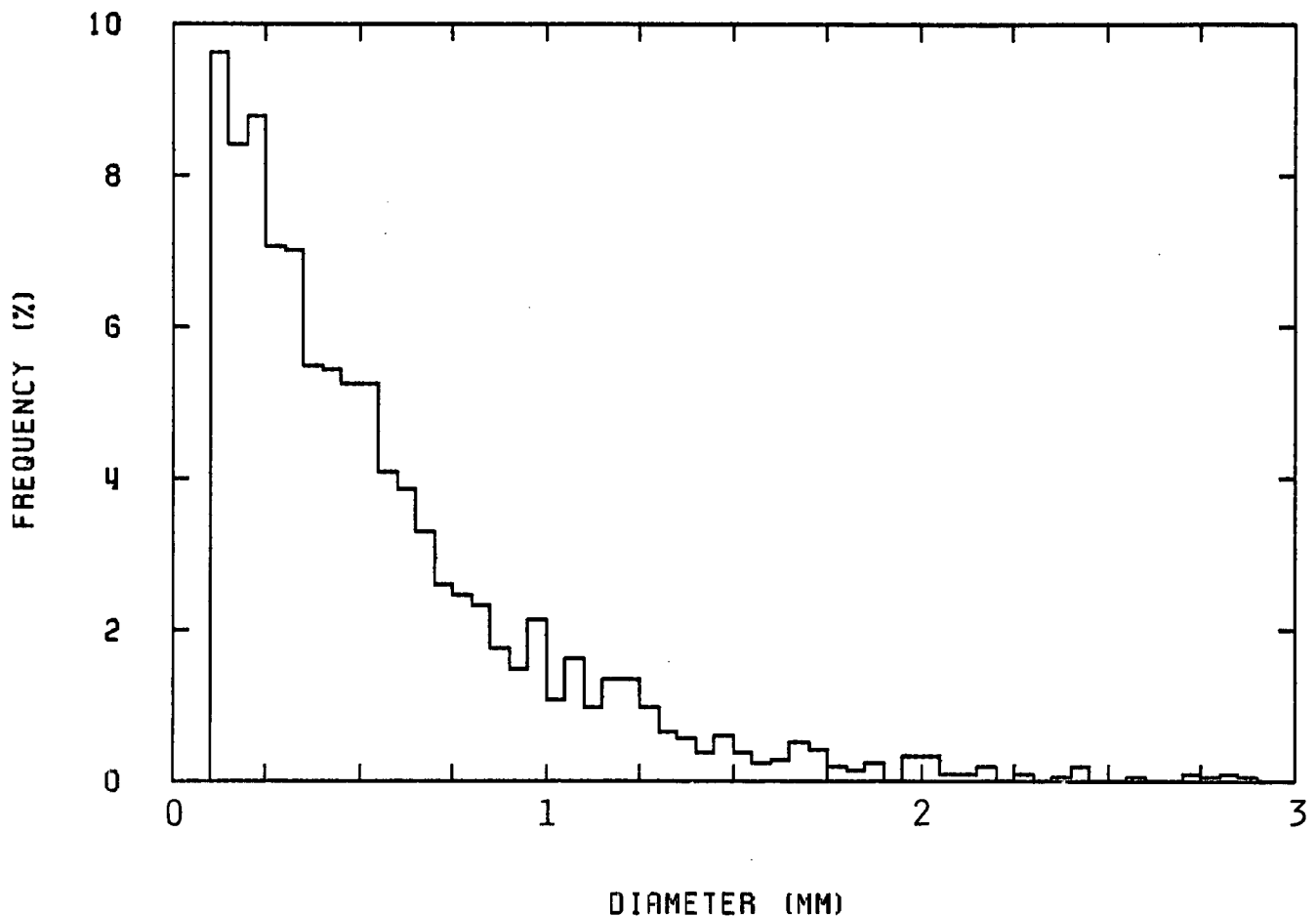


Figure 10. Droplet Size Distribution at the Nacelle Inlet Plane

REFERENCES

1. Murthy, S.N.B. and C.M. Ehresman: Effects of Water Ingestion into Jet Engine. AIAA paper No. 84-0542 presented at the Airbreathing Propulsion Session of the 22nd Aerospace Sciences Meeting, January 1984.
2. Murthy, S.N.B. et.al.: A Stagnation Pressure Probe for Droplet-laden Air Flow. AIAA paper No. 85-0330 presented at the Airbreathing Propulsion Session of the 23rd Aerospace Sciences Meeting, January 1985.
3. Code of Federal Regulations, Title 14-Aeronautics and Space, Chapter 1-Federal Aviation Administration, Article 33.77, paragraphs (c) and (f). January 1980.
4. Code of Federal Regulations, Title 14-Aeronautics and Space, Chapter 1-Federal Aviation Administration, Article 25.1091, paragraph (d)(2). January 1980.
5. Barrett, R.V.: Spray From Aircraft Undercarriages at High Speed - a Model Investigation. The Aeronautical Journal, Royal Aeronautical Society, May 1977.
6. Jones, A.R.: A Review of Drop Size Measurement - The Application of Techniques to Dense Fuel Sprays. Progress in Energy and Combustion Science. Vol. 3. 1977.
7. McCreath, C.G. and J.M. Beer: A Review of Drop Size Measurement in Fuel Sprays. Applied Energy, Vol. 2. 1976.
8. Gardiner, J.A.: Measurement of the Drop Size Distribution in Water Sprays by an Electrical Method. Instrument Practice. April 1964.

APPENDIX A
IMAGE ANALYSIS PROGRAMS

FORTRAN IV-P V82-51 10:58:17 26-APR-85 P 1
 DROPS.FTH /TR:BLOCKS/WR

```

0001      PROGRAM DROPS
C
C      Drops analysis based on averaged maximum gradient
C
0002      LOGICAL*1 ANSA,AN30
0003      BYTE ZERO
0004      REAL*8 HIST(0:255),DMAXO
0005      BYTE BUPIC(512),BUGRA(512)
0006      BYTE PIXEL(512,16)
0007      COMMON/PINTA/PIXEL
0008      INTEGER*2 IVLT(256)
0009      INTEGER*2 ARMIN
0010      INTEGER*2 IBUFO(8) ! Basic data processing parameters
0011      EQUIVALENCE (IBUFO(1),KREDC)
0012      EQUIVALENCE (IBUFO(2),SCALE)
0013      EQUIVALENCE (IBUFO(4),ARMIN)
0014      EQUIVALENCE (IBUFO(5),ICORTA)
0015      INTEGER*2 SL,SS,NL,NS
0016      REAL*4 ABUF(200),PBUF(200)
0017      INTEGER*2 LIMIT(4,200)
0018      COMMON/MINARE/AMINAR
0019      INTEGER*2 IBUFE(8),PL,PC,CL,CC
0020      REAL*4 AREA,PERIM
0021      EQUIVALENCE (IBUFE(1),PL)
0022      EQUIVALENCE (IBUFE(2),PC)
0023      EQUIVALENCE (IBUFE(3),CL)
0024      EQUIVALENCE (IBUFE(4),CC)
0025      EQUIVALENCE (IBUFE(5),AREA)
0026      EQUIVALENCE (IBUFE(7),PERIM)
C
C      Open data file
C
0027      OPEN (UNIT=3,NAME='SY:[300,300]RAIN.DAT',TYPE='OLD',
1 DISP='KEEP',ACCESS='DIRECT',RECORDSIZE=4,FORM='UNFORMATTED')
0028      READ(3'1') IBUFO
0029      IF (KREDC.NE.0) GO TO 900
0030      KREDC=11 Initial record for parameters storage,no data
0031      ARMIN=51 Default min area
0032      ICORTA=5
0033      SCALE=1
0034      TYPE *,' Processing parameters initialization, defaults are:'
0035      TYPE *,' Min area 5 Sq. pixels, Scale 1 mm/pixel; Change (Y/N)?'
0036      ACCEPT 101,ANSA
0037      IF (ANSA.NE.'Y') GO TO 111
0038      TYPE *,' Enter Min area (Sq. pix) and Scale (mm/pix)'
0039      ACCEPT *,ARMIN,SCALE
0040      GO TO 111
0041      900      TYPE *,' File has already data, Stops execution (Y/N)?'
0042      ACCEPT 101,ANSA
0043      IF (ANSA.EQ.'Y') GO TO 950
C
C      First detector
C
0044      111      TYPE *,' Begin coarse detection'

```

ORIGINAL PAGE IS
OF POOR QUALITY

FORTRAN IV-A 3 V82-51 10:50:17 26-APR-85 | 2
DROPS.FTN /TR:BLOCKS/WR

0045 CALL SETUP
0046 TYPE *, ' Smoothing before compute gradient (Y/N)'
0047 ACCEPT 101,ANSA
0048 IF (ANSA.EQ.'N') GO TO 4
0049 CALL SMOOTH
0050 GO TO 5
0051 4 DO 3 K=1,256
0052 3 IVLT(K)=K/2
0053 CALL VLTCUR(1,IVLT)
C
C Save original picture
C
0054 5 CALL SETUP
0055 OPEN (UNIT=7,TYPE='SCRATCH',ACCESS='DIRECT',INITIALSIZE=512,
I RECORDSIZE=128)
0056 NBLK=1
0057 DO 10 K=1,32
0058 LIN=(K-1)*16+1
0059 ICOD=IMAGE(8,LIN,16,'R',PIXEL)
0060 ISTAT=JESC(7,PIXEL,NBLK,4096,1,NBLK)
0061 10 CONTINUE
C
C Transfer smooth picture to channel 8
C
0062 CALL SETUP
0063 CALL INSEL(2,8,8)
0064 CALL OUTNBL(1)
0065 CALL FMOPER
C
C Compute gradient
C
0066 CALL SETUP
0067 CALL GRADIE
C
C Restore original picture
C
0068 CALL SETUP
0069 NBLK=1
0070 DO 20 K=1,32
0071 LIN=(K-1)*16+1
0072 ISTAT=JLEE(7,PIXEL,NBLK,4096,1,NBLK)
0073 ICOD=IMAGE(8,LIN,16,'W',PIXEL)
0074 20 CONTINUE
C
C Threshold gradient picture
C
0075 CALL SETUP
0076 CALL INSEL(1,8,8)
0077 CALL OUTNBL(4)
0078 CALL FMOPER
0079 CALL SETUP
0080 50 TYPE *, ' Threshold gradient image',ICORTA
0081 CALL SETUP
0082 DO 51 JLT=1,ICORTA
0083 51 IVLT(JLT)=JLT
0084 DO 52 JLT=ICORTA+1,256

FORTRAN IV-	S	V02-51	10:50:17	26-APR-85	E 3
DROPS.FTH		/TR:BLOCKS/WR			
0085	52	IVLT(JLT)=255			
0086		CALL VIDTHR(1,IVLT)			
0087		TYPE *, 'Accept threshold (y/n)'			
0088		ACCEPT 101,AHSA			
0089		IF (AHSA.NE.'N') GO TO 60			
0090		TYPE *, 'Enter gradient image threshold'			
0091		ACCEPT *,ICORTA			
0092		GO TO 50			
0093	101	FORMAT(A1)			
0094	60	CALL SETUP			
0095		DO 70 JLT=ICORTA+1,256			
0096	70	IVLT(JLT)=JLT-1			
0097		CALL VLTCK(1,IVLT)			
0098		CALL SETUP			
	C				
	C	Save gradient picture			
	C				
0100		NBLK=1			
0101		DO 80 K=1,32			
0102		LIN=(K-1)*16+1			
0103		ICOD=IMAGE(1,LIN,16,'R',PIXEL)			
0104	80	ISTAT=JESC(7,PIXEL,NBLK,4096,1,NBLK)			
	C	CONTINUE			
	C				
	C	Remove background variations			
	C				
0105		TYPE *, 'Remove background variations (Y/N)'			
0106		ACCEPT 101,AHSD			
0107		IF (AHSD.NE.'N') GO TO 85			
0108		CALL INSEL(2,8,B)			
0109		CALL OUTNBL(4)			
0110		CALL FMOPER			
0111		CALL SETUP			
0112		CALL INSEL(1,8,B)			
0113		CALL OUTNBL(2)			
0114		CALL FMOPER			
0115		CALL SETUP			
0116		GO TO 80			
0117	85	ISD=100 / Variations scale			
0118		CALL HIGPASK(ISD,1,B)			
0119		CALL SETUP			
	C				
	C	Restore gradient picture			
	C				
0120		NBLK=1			
0121		DO 120 K=1,32			
0122		LIN=(K-1)*16+1			
0123		ISTAT=JLEE(7,PIXEL,NBLK,4096,1,NBLK)			
0124		ICOD=IMAGE(2,LIN,16,'W',PIXEL)			
0125	120	CONTINUE			
	C				
	C	Compute Histogram			
	C				
0126	80	ZERO='0'			
0127		TYPE *, ' Computing modified PDF '			
0128		DO 90 K=0,255			

```
0129      90      HIST(K)=0.  
0130      DO 150 K=10,500  
0131      ICOD=IMAGE(1,K,1,'R',BUPIC)  
0132      ICOD=IMAGE(2,K,1,'R',BUGRA)  
0133      DO 150 J=10,500  
0134      IF (BUGRA(J).EQ.ZERO) GO TO 150  
0135      A=IV(BUGRA(J))  
0136      I1=IV(BUPIC(J))  
0137      HIST(I1)=HIST(I1)+I1*A  
0138      150      CONTINUE  
C  
C      Display histogram and threshold determination  
C  
0139      DMAXO=0.  
0140      DO 180 K=0,255  
0141      IF (HIST(K).GT.DMAXO) DMAXO=HIST(K)  
0142      180      CONTINUE  
0143      DO 182 K=0,255  
0144      HIST(K)=HIST(K)/DMAXO  
0145      182      CONTINUE  
0146      CALL INSEL(1,0,0)  
0147      CALL OUTNBL(4)  
0148      CALL FMOPER  
0149      CALL SETUP  
0150      DO 160 K=1,256  
0151      160      IVLT(K)=0  
0152      CALL VIDTHR(1,IVLT)  
0153      ITHR=0  
0154      CALL DISHS(HIST,ITHR)  
0155      TYPE *, ' Enter (1) simple, (2) bimodal distribution'  
0156      ACCEPT *, IMODES  
0157      CALL SEUDIS(HIST,ITHR,IMODES)  
0158      300      TYPE *, ' Estimated threshold', ITHR  
0159      CALL SETUP  
0160      DO 391 JLT=1,ITHR  
0161      391      IVLT(JLT)=0  
0162      DO 392 JLT=ITHR+1,256  
0163      392      IVLT(JLT)=255  
0164      CALL VLTORG(1,IVLT)  
0165      CALL SETUP  
0166      IVLT(1)=0  
0167      IVLT(256)=1  
0168      CALL VLTORG(1,IVLT)  
0169      CALL SETUP  
0170      CALL BORDEA(IVLT)  
0171      CALL SETUP  
0172      CALL DISHS(HIST,ITHR)  
0173      TYPE *, ' Accept threshold (Y/N)'  
0174      ACCEPT 101,ANS1  
0175      IF (ANS1.NE.'N') GO TO 350  
0176      TYPE *, ' Enter threshold'  
0177      ACCEPT *, ITIR  
0178      IF (ANS1.NE.'N') GO TO 320  
0179      CALL INSEL(1,0,0)  
0180      CALL OUTNBL(2)  
0181      CALL FMOPER
```

ORIGINAL PAGE IS
OF POOR QUALITY

FORTRAN IV-
 DROPS.FTN- S VMS-51 10:50:17 26-APR-85 P E 5
 /TR:BLOCKS/WR

```

0102      CALL SETUP
0103      GO TO 300
0104      320  CALL HIGHPASS( ISD,1,0 )
0105      CALL SETUP
0106      GO TO 300
0107      350  TYPE *, ' Default region the entire picture; change (Y/N)'
0108      ACCEPT 101,AHSA
0109      IF (AHSA.EQ.'Y') GO TO 400
0110      SL=1
0111      SS=1
0112      NL=510
0113      NS=510
0114      GO TO 450
0115      400  TYPE *, ' Use cursor to define region/push white key'
0116      CALL REGION(SL,SS,NL,NS)
0117      C
0118      450  AMINAR=ARMIN
0119      TYPE *, ' Region definition SL=',SL,' SS=',SS,' NL=',NL,' NS=',NS
0120      IVLT(1)=0
0121      IVLT(2)=255
0122      IVLT(256)=255
0123      CALL VLTCOR(1,IVLT)
0124      CALL SETUP
0125      TYPE *, ' Computing drops size'
0126      CALL GOTAS(1,SL,SS,NL,NS,ABUF,PBUF,LIMIT,NUMOBJ)
0127      IVLT(1)=0
0128      IVLT(256)=1
0129      CALL VLTCOR(1,IVLT)
0130      CALL BORDEA(IVLT)
0131      CALL SETUP
0132      TYPE *, ' End coarse detector'
0133      CLOSE(UNIT=7)
0134      C
0135      C     Save results on disk
0136      C
0137      2000  NUMDR=0
0138      SCALE2=SCALE*SCALE
0139      TYPE *, ' DATABASE: Initial element',KREDC
0140      DO 2001 K=1,NUMOBJ
0141      NUMDR=NUMDR+1
0142      KREDC=KREDC+1
0143      PL=LIMIT(1,K)
0144      PC=LIMIT(2,K)
0145      CL=LIMIT(3,K)
0146      CC=LIMIT(4,K)
0147      AREA=ABUF(K)*SCALE2
0148      PERIM=PBUF(K)*SCALE
0149      WRITE(3,'(KREDC)') IBUFE
0150      IF (KREDC.EQ.1281) GO TO 2025
0151      CONTINUE
0152      2001  TYPE *, ' DATABASE: Final element',KREDC-1
0153      TYPE *, ' Number of objects in this frame',NUMDR
0154      WRITE(3,'(1)') IBUF0!Update general information record
0155      950  CLOSE(UNIT=3)
0156      END
  
```

ORIGINAL PAGE IS
OF POOR QUALITY

FORTRAN, IV-PL V92-51 14:09:02 25-APR-85 PA 1
GOTAS.FTN /TR:BLOCKS/WR

0001 SUBROUTINE GOTAS(CHAN,SL,SS,NL,NS,ABUF,PBUF,LIMIT,NUMOBJ)
C
C Drops geometrical characterization
C
0002 INTEGER*2 CHAN,SL,SS,NL,NS
0003 BYTE PIXEL(512,16)
0004 COMMON /PINTA/PIXEL
0005 INTEGER*2 FLAG(512,2),ID(30)
0006 INTEGER*2 ISLG(90),ISSS(90),EL(90),ES(90)
0007 INTEGER*2 CNTR(90,2),BEGIN(90,2),IEND(90,2)
0008 INTEGER*2 OLDID,NEWID
0009 INTEGER*4 NPIXG(90)
0010 REAL*4 RPER(90)
0011 REAL*4 ABUF(1),PBUF(1)
0012 INTEGER*2 LIMIT(4,1)
C
C Initialize
C
0013 CALL ZIA(FLAG(1,1),1024)
0014 CALL ZIA(RPER,100)
0015 CALL ZIA(NPIXG,100)
0016 CALL ZIA(EL,90)
0017 CALL ZIA(ES,90)
0018 CALL ZIA(CNTR(1,1),100)
0019 CALL ZIA(BEGIN(1,1),100)
0020 CALL ZIA(IEND(1,1),100)
0021 CALL ITIA(32000,ISLG,90)
0022 CALL ITIA(32000,ISSS,90)
0023 NUMOBJ=0
0024 ISW=1
0025 NEWC=0
0026 NOLC=0
0027 OLDID=1
0028 NSS=SS+NS
0029 NSL=SL-1
0030 HLL=HSL+NL
C
C Main loop
C
0031 DO 100 L=1,NL,16
0032 IBLOCK=MIN0(16,NL-L)
0033 LINE=L+NSL
0034 ICOD=IMAGE(CHAN,LINE,IBLOCK,'R',PIXEL)
0035 DO 100 KK=1,16
0036 H1=SS
0037 LINIA=LINE+KK-1
0038 NEWC=0 ! Start searching for an object gt 0
0039 105 DO 110 J=H1,NSS ! look for left edge
0040 IF (.NOT.PIXEL(J,KK)) GO TO 120
0041 110 CONTINUE
C No more edges on this line
0042 GO TO 103
0043 120 H1=J ! Left edge
0044 DO 130 J=H1,NSS ! Look right edge
0045 IF (.NOT.PIXEL(J,KK)) GO TO 140
0046 130 CONTINUE

ORIGINAL PAGE IS
OF POOR QUALITY

FORTRAN IV-PL GOTAS.FTN	V02-51 TR:BLOCKS/WR	14:09:02	25-APR-05	PA 12
0047		J=NSS+1 ! Right edge is the picture boundary		
0048	140	H2=J-1		
	C			
	C	Find ID of this object from previous flag line		
	C			
0049		CALL MATCH(FLAG(1,3-ISW),N1,N2,NUM,ID,NSS)		
0050		NEWID=ID(1)		
0051		IF (NUM.LT.2) GO TO 101		
	C			
	C	If many ID condense them into one		
0052		CALL CONID(RPER,NPIXS,ISLS,ISSS,EL,ES,NUM,ID)		
0053		GO TO 102		
0054	101	IF (NUM.NE.0) GO TO 102		
	C			
	C	If there is not ID them creates one		
0055		CALL FIND(90,NEWID,NPIXS,OLDID)		
	C			
0056		begin counting perimeter new object		
	C	RPER(NEWID)=N2-N1+2		
	C			
0057	102	And update flag buffer and counters		
0058		CALL ITIA(NEWID,FLAG(N1,ISW),H2-N1+1)		
0059		HEWC=HEWC+1		
0060		CNTR(HEWC,ISW)=NEWID		
0061		BEGIN(HEWC,ISW)=N1		
	C			
	C	IEND(HEWC,ISW)=N2		
0062		Update statistics buffer		
0063		NPIXS(NEWID)=NPIXS(NEWID)+N2-N1+1		
0064		IF ((ISLS(NEWID)).GT.LINIA) ISLS(NEWID)=LINIA		
0065		IF ((ISSS(NEWID)).GT.N1) ISSS(NEWID)=N1		
0066		IF (ES(NEWID)).LT.N2) ES(NEWID)=N2		
0067		EL(NEWID)=LINIA		
	C			
	C	CALL PERIM(HOLC,HEWC,CNTR(1,ISW),NEWID,RPER,BEGIN(1,3-ISW), I BEGIN(1,ISW),IEND(1,3-ISW),IEND(1,ISW))		
	C			
0068		Send back for more data on the same line		
0069		H1=N2+2		
	C			
	C	IF (H1.LE.NSS) GO TO 105		
	C			
	C	Search buffers for terminated drops		
0070	103	CALL ENOFLIC(RPER,NPIXS,ISLS,ISSS,EL,ES,NLL,LINIA,CNTR(1,3-ISW), 1 CNTR(1,ISW),HOLC,HEWC,NUMOBJ,BEGIN(1,3-ISW),BEGIN(1,ISW), 2 IEND(1,3-ISW),IEND(1,ISW),ABUF,PBUF,LIMIT)		
0071		CALL ZIA(FLAG(1,3-ISW),512) ! Zero flag line		
0072		ISW=3-ISW ! Switch the flag		
0073		HOLC=HEWC		
0074	100	CONTINUE ! Close main loop		
0075		RETURN		
0076		END		

FORTRAN-IV-P V92-51 19:01:38 84-APR-85
MATCH.FTN /TR:BLOCKS/WR

P 1

0001 SUBROUTINE MATCH(FLAG,N1,N2,NUM,ID,NS)
C
C RETURN I.D. OF OBJECT FOUND ON PREVIOUS LINE
C FLAG = OLD FLAG BUFFER
C N1 = BEGIN, N2 = END OF OBJECT
C NUM = NUMBER OF OBJECTS LOCATED
C ID = I.D. OF OBJECTS LOCATED
0002 INTEGER FLAG(1)
0003 INTEGER*4 ID(1)
0004 M1 = N1 - 1
0005 M2 = N2 + 1
0006 IF (M1.LT.1) M1 = 1
0007 IF (M2.GT.NS) M2=NS
0008 NUM = 0
0009 K = 0
C
C FIND ALL FLAGS
C
0010 DO 10 J=M1,M2
0011 IF (FLAG(J).EQ.K) GO TO 10
0012 IF (FLAG(J).EQ.0) GO TO 10
0013 K = FLAG(J)
0014 NUM = NUM + 1
0015 ID(NUM) = K
0016 10 CONTINUE
0017 IF (NUM.LT.2) RETURN
C
C REJECT DUPLICATES
C
0018 CALL CORSRT(ID, ID, NUM)
0019 N = 1
0020 K = ID(1)
0021 DO 20 J=2,NUM
0022 IF (K.EQ.ID(J)) GO TO 20
0023 N = N + 1
0024 ID(N) = ID(J)
0025 20 CONTINUE
0026 NUM = N
0027 RETURN
0028 END

ORIGINAL PAGE IS
OF POOR QUALITY

FORTRAN IV-T V02-51 19:81:84 84-APR-85 P 1
PERIM.FTH /TR:BLOCKS/VR

```

8001      SUBROUTINE PERIM(NOLC,NEWC,NECNTR,NEWID,RPER,OBEGIN,NBEGIN,
     1          OEND,NEND)
C
C      THIS SUBROUTINE ACCUMULATES PERIMETER MEASUREMENTS FOR THE 'OLD'
C      LINE BETWEEN N1 AND N2 OF THE 'NEW' LINE.
C
8002      INTEGER NECNTR(1),OBEGIN(1),NBEGIN(1),OEND(1),NEND(1)
8003      REAL*4 RPER(1)
8004      IF (NOLC.EQ.0) RETURN
C
C      SEARCH 'OLD' LINE FOR MATCHING OBJECT SEGMENTS.
C
8005      L1 = 0
8006      DO 100 J=1,NOLC
8007      IF (OEND(J).GE.NBEGIN(NEWC)-1.AND.
     1          OBEGIN(J).LE.NEND(NEWC)+1) GO TO 101
8008      GO TO 100
8009      101  ONEWC = NEWC - 1
8010      IF (ONEWC.LT.1) GO TO 301
8011      IF (NEWID.EQ.NECNTR(ONEWC).AND.OEND(L2).GE.NBEGIN(NEWC))
     1          GO TO 302
8012      GO TO 301
C
C      IF PERIMETER HAS BEEN ADDED FOR PREVIOUS PARTICLE SEGMENT ON
C      'NEW' LINE WITH SAME I.D. AND THE 'OLD' MATCHING SEGMENT
C      OVERLAPS BOTH 'NEW' SEGMENTS, THEN THE OVERLAP IN THE
C      CURRENT SEGMENT IS SUBTRACTED FROM THE PERIMETER VALUE.
C
8013      302  RPER(NEWID) = RPER(NEWID) - SQRT((OEND(L2)
     1          - FLOAT(NEND(ONEWC)))**2 + 1.) + NBEGIN(NEWC) - NEND(ONEWC)
8014      GO TO 303
8015      301  RPER(NEWID) = RPER(NEWID) + SQRT((NBEGIN(NEWC)
     1          - FLOAT(OBEGIN(J)))**2 + 1.)
8016      303  L1 = J
8017      K = J + 1
8018      GO TO 102
8019      100  CONTINUE
8020      102  IF (L1.EQ.0) RETURN
8021      L2 = J
8022      IF (K.GT.NOLC) GO TO 200
8023      DO 103 J=K,NOLC
8024      IF (OEND(J).GE.NBEGIN(NEWC)-1.AND.
     1          OBEGIN(J).LE.NEND(NEWC)+1) GO TO 104
8025      GO TO 103
8026      104  RPER(NEWID) = RPER(NEWID) + (OBEGIN(J) - OEND(J-1))
8027      L2 = J
8028      103  CONTINUE
8029      200  IF (L2.EQ.0) L2 = L1
8030      RPER(NEWID) = RPER(NEWID) + SQRT((NEND(NEWC)
     1          - FLOAT(OEND(L2)))**2 + 1.)
8031      RETURN
8032      END

```

FORTRAN IV-
CONID.FTN

6 V82-51
/TR:BLOCKS/WR

18:59:52 84-APR-85

[1

0001 SUBROUTINE CONID(RPER,NPIXS,ISLS,ISSS,EL,ES,NUM,ID)
C
C USED TO CONCATINATE MANY I.D.'S
C
0002 INTEGER OLDID,ISLS(1),ISSS(1),EL(1),ES(1)
0003 INTEGER*4 NPIXS(1),ID(1)
0004 REAL*4 RPER()
0005 NEWID = ID(1)
0006 DO 10 J=2,NUM
0007 OLDID = ID(J)
0008 RPER(NEWID) = RPER(NEWID) + RPER(OLDID).
0009 RPER(OLDID) = 0.
0010 NPIXS(NEWID) = NPIXS(NEWID) + NPIXS(OLDID)
0011 NPIXS(OLDID) = 0
0012 IF (ISLS(NEWID).GT.ISLS(OLDID)) ISLS(NEWID) = ISLS(OLDID)
0013 ISLS(OLDID) = 32000
0014 IF (ISSS(NEWID).GT.ISSS(OLDID)) ISSS(NEWID) = ISSS(OLDID)
0015 ISSS(OLDID) = 32000
0016 IF (EL(NEWID).LT.EL(OLDID)) EL(NEWID) = EL(OLDID)
0017 EL(OLDID) = 0
0018 IF (ES(NEWID).LT.ES(OLDID)) ES(NEWID) = ES(OLDID)
0019 10 ES(OLDID) = 0
0020 RETURN
0021 END

FORTRAN IV-P V82-51 19:02:52 84-APR-85 P 1
PCNCAT.FTN /TR:BLOCKS/WR

8881 SUBROUTINE PCNCAT(NCEN,PCNTR,BEGIN,END,NEWID,RPER)
C THIS SUBROUTINE CONCATINATES ALL ENDING PERIMETER VALUES FOR EACH
C I.D. ON AN ENDING LINE.
C
8882 INTEGER PCNTR(1),BEGIN(1),END(1)
8883 REAL*4 RPER(1)
8884 DO 100 J=1,NCEN
8885 IF (NEWID.EQ.PCNTR(J)) GO TO 101
8886 GO TO 100
8887 101 RPER(NEWID) = RPER(NEWID) + END(J) - BEGIN(J) + 2.
8888 100 CONTINUE
8889 RETURN
8890 END

FORTRAN IV-P
FIND.FTN

V92-51
/TR:BLOCKS/WR

19:03:00

04-APR-85

P 1

0001 SUBROUTINE FIND(NBIN,NEWID,NPIXS,OLDID)
C
C USED TO FIND A NEW BIN POSITION
C NBIN = LENGTH OF BIN BUFFERS
C NEWID = NEW BIN VALUE RETURNED
C NPIXS = SUM OF PIXELS BUFFER
C OLDID = LAST FOUND I.D.
0002 INTEGER OLDID
0003 INTEGER*4 NPIXS(1)
0004 DO 100 J=OLDID,NBIN
0005 IF (NPIXS(J).EQ.0) GO TO 200
0006 100 CONTINUE
0007 DO 150 J=1,OLDID
0008 IF (NPIXS(J).EQ.0) GO TO 200
0009 150 CONTINUE
0010 TYPE *, ' All bins filled'
0011 STOP
0012 200 NEWID=J
0013 OLDID=J
0014 RETURN
0015 END

FORTRAN IV-P V92-51 19:03:28 84-APR-85
CORSRT.FTN /TR:BLOCKS/VR

P 1

0001 SUBROUTINE CORSRT(KEY,PTR,LEN)

C IN CORE SORT ROUTINE. SORTS THE VECTORS KEY AND PTR INTO ASCENDING ORDER OF
C KEY. THE VALUES IN KEY ARE TREATED AS LOGICAL QUANTITIES HENCE SIGN BITS
C MUST BE TREATED ACCORDINGLY. ALPHABETIC RECORDS MAY BE SORTED SINCE
C CHARACTER CODES ARE IN LOGICAL ORDER. THE PTR ARRAY CAN THEN BE USED TO MOV
C RECORDS IN A DISK FILE.

C

IMPLICIT INTEGER(A-Z)
INTEGER*4 IMSK,JMSL,SM(32),PTR(1),TEMP
LOGICAL*4 IMSL,JMSL,KEY(1),LTEMP
DIMENSION BDRY(3,32),CBD(32)
EQUIVALENCE (IMSK,IMSL),(JMSK,JMSL)
DATA SM(1),SM(2),SM(17)/020000000000,010000000000,01000000/
C

DO 1 I=3,16
1 SM(I) = SM(I-1)/2
DO 2 I=10,32
2 SM(I) = SM(I-1)/2
LEV = 1
BDRY(2,LEV) = 1
BDRY(3,LEV) = LEN
CBD(LEV) = 2
CB = CBD(LEV)
PL = BDRY(CB,LEV)
PU = BDRY(CB+1,LEV)
IF (PL.GE.PU) GO TO 75
IMSK = SM(LEV)
JMSL = KEY(PL).AND. IMSL
IF (JMSK.NE.0) GO TO 85
PL = PL + 1
IF (PL.EQ.PU) GO TO 73
GO TO 81
JMSL = KEY(PU).AND. IMSL
IF (JMSL.NE.0) GO TO 86
LTEMP = KEY(PL)
TEMP = PTR(PL)
KEY(PL) = KEY(PU)
PTR(PL) = PTR(PU)
KEY(PU) = LTEMP
PTR(PU) = TEMP
GO TO 81
PU = PU - 1
IF (PU.NE.PL) GO TO 85
JMSL = KEY(PL).AND. IMSL
IF (JMSL.NE.0) PL = PL - 1
IF (LEV.GE.32) GO TO 75
CB = CBD(LEV)
LEV = LEV + 1
CBD(LEV) = 1
BDRY(1,LEV) = BDRY(CB,LEV-1)
BDRY(2,LEV) = PL
BDRY(3,LEV) = BDRY(CB+1,LEV-1)
GO TO 72
IF (CBD(LEV).EQ.2) GO TO 76
CBD(LEV) = 2

FORTRAN-IV-P
CORSRT.FTN

V02-51
/TR:BLOCKS/WR

19:03:28 84-APR-85

P 2

0049 BDRY(2,LEV) = BDRY(2,LEV) + 1
0050 GO TO 72
0051 76 LEV = LEV - 1
0052 IF (LEV.GT.0) GO TO 75
0053 RETURN
0054 END

FORTRAN-IV-P
ENOFLI.FTN,

V92-51 19:01:54 84-APR-85

P 1

0001 SUBROUTINE ENOFLI(RPER,NPIXS,ISLS,ISSS,EL,ES,NL,LINE,
1 OLCNTR,NECNTR,NOLC,NEWC,NUM,OBEGIN,NBEGIN,
2 OEND,NEND,ABUF,PBUF,LIMIT)
C
C SEARCH FOR FINISHED OBJECTS
C
0002 INTEGER*4 NPIXS()
0003 INTEGER OLCNTR(),NECNTR(),OBEGIN(),NBEGIN(),OEND(),NEND()
0004 INTEGER ISLS(),ISSS(),EL(),ES()
0005 REAL*4 RPER(),ABUF(),PBUF()
0006 INTEGER*2 LIMIT(4,1)
C
C SEARCH OLCNTR FOR I.D.'S NOT IN NECNTR
C
0007 IF (LINE.EQ.NL) GO TO 52
0008 IF (NOLOC.EQ.0) RETURN
0009 IF (NEWC.EQ.0) GO TO 51
0010 DO 10 J=1,NOLOC
0011 NEWID = OLCNTR(J)
0012 DO 20 K=1,NEWC
0013 IF (NEWID.EQ.NECNTR(K)) GO TO 10
0014 20 CONTINUE
C
C DROPLET NOT CONTINUED
C
0015 CALL PCNCAT(NOLC,OLCNTR,OBEGIN,OEND,NEWID,RPER)
0016 CALL FINAL(NEWID,RPER,NPIXS,ISLS,ISSS,EL,ES,NUM,ABUF,
1 PBUF,LIMIT)
0017 10 CONTINUE
0018 RETURN
C
C FINISH OFF EVERYTHING
C
0019 51 DO 50 J=1,NOLOC
0020 NEWID = OLCNTR(J)
0021 CALL PCNCAT(NOLC,OLCNTR,OBEGIN,OEND,NEWID,RPER)
0022 CALL FINAL(NEWID,RPER,NPIXS,ISLS,ISSS,EL,ES,NUM,ABUF,
1 PBUF,LIMIT)
0023 50 CONTINUE
0024 RETURN
0025 52 IF (NOLOC.EQ.0) GO TO 60
0026 IF (NEWC.EQ.0) GO TO 51
0027 DO 60 J=1,NOLOC
0028 NEWID = OLCNTR(J)
0029 DO 90 K=1,NEWC
0030 IF (NEWID.EQ.NECNTR(K)) GO TO 100
0031 90 CONTINUE
0032 CALL PCNCAT(NOLC,OLCNTR,OBEGIN,OEND,NEWID,RPER)
0033 CALL FINAL(NEWID,RPER,NPIXS,ISLS,ISSS,EL,ES,NUM,ABUF,
1 PBUF,LIMIT)
0034 100 GO TO 60
0035 100 CALL PCNCAT(NEWC,NECNTR,NBEGIN,NEND,NEWID,RPER)
0036 CALL FINAL(NEWID,RPER,NPIXS,ISLS,ISSS,EL,ES,NUM,ABUF,
1 PBUF,LIMIT)
0037 60 CONTINUE
0038 RETURN

FORTRAN:IV-P
ENOFI.FTN

V02-51
/TR:BLOCKS/WR

19:01:54

04-APR-85

P 2

```
0039      60  IF (NEWC.EQ.0) RETURN
0040      DO 70 J=1,NEWC
0041      NEWID = NECNTR(J)
0042      CALL PCNCAT(NEWC,NECNTR,NBEGIN,NEND,NEWID,RPER)
0043      CALL FINAL(NEWID,RPER,NPIXS,ISLS,ISSS,EL,ES,NUM,ABUF,
1          PBUF,LIMIT)
0044      70  CONTINUE
0045      RETURN
0046      END
```

```
0001      SUBROUTINE FINAL(NEWID,RPER,NPIXS,ISLS,ISSS,EL,ES,NUM,ABUF,
1                  PBUF,LIMIT)
C
C      TO TERMINATE AN OBJECT
C
0002      INTEGER*4 NPIXS(1)
0003      INTEGER*2 LIMIT(4,1)
0004      INTEGER ISLS(1),ISSS(1),EL(1),ES(1)
0005      REAL*4 RPER(1),ABUF(1),PBUF(1)
0006      BYTE ORIGA(512)
0007      COMMON /MINARE/ AMINAR
0008      IF (NPIXS(NEWID).EQ.9) RETURN
0009      NUM = NUM + 1
0010      IF (NUM.LT.201) GO TO 5
0011      TYPE *, ' Number of spots gt buffer space available'
0012      STOP
C
C      ACCUMULATE DROPLET STATISTICS
C
0013      5      ABUF(NUM) = NPIXS(NEWID)
0014      PBUF(NUM) = RPER(NEWID)
0015      LIMIT(1,NUM) = ISLS(NEWID)
0016      LIMIT(2,NUM) = ISSS(NEWID)
0017      LIMIT(3,NUM) = EL(NEWID) - ISLS(NEWID) + 1
0018      LIMIT(4,NUM) = ES(NEWID) - ISSS(NEWID) + 1
C      CLEAR OUT BINS
0019      IF (ABUF(NUM).GT.AMINAR) GO TO 10
0020      CALL BORRAR(1,LIMIT(1,NUM),LIMIT(2,NUM),LIMIT(3,NUM),LIMIT(4,NUM))
0021      NUM=NUM-1
C
0022      10      NPIXS(NEWID) = 0
0023      RPER(NEWID) = 0.
0024      ISLS(NEWID) = 32000
0025      ISSS(NEWID) = 32000
0026      EL(NEWID) = 0
0027      ES(NEWID) = 0
0028      RETURN
0029      END
```

APPENDIX B
DROPLET STATISTICS PROGRAM

FORTRAN IV-P
 RAINST.FTN V02-51 10:58:38 23-FEB-84 P 1
 /TR:BLOCKS/VR

0001 PROGRAM RAINST
 C
 C Road droplets' data file and compute general statistic
 C
 C Programmer: Miguel A. Hernan
 C

```

0002 REAL*4 DBUF(1200),VOBUF(1200),ESFER(1200)
0003 REAL*8 SHD3,SHD2,DTOT,ESTOT,SMD4,COMUD
0004 INTEGER*2 NUHE
0005 LOGICAL*1 ANSA
0006 REAL*4 VOLHIS(0:79),FREHIS(0:79)
0007 REAL*4 AREA,PERIM,D3,D2,D,D4
0008 LOGICAL*1 NOZOD(12),NOZIN(68),NOZID(88)
0009 EQUIVALENCE(NOZOD(1),NOZID(1))
0010 EQUIVALENCE(NOZIN(1),NOZID(13))
0011 INTEGER*2 OPEPLO
0012 LOGICAL*1 FILEAC(22)
0013 INTEGER*2 IBUFER(0),SL,SS,NL,NS
0014 EQUIVALENCE(IBUFER(1),SL)
0015 EQUIVALENCE(IBUFER(2),SS)
0016 EQUIVALENCE(IBUFER(3),NL)
0017 EQUIVALENCE(IBUFER(4),NS)
0018 EQUIVALENCE(IBUFER(5),AREA)
0019 EQUIVALENCE(IBUFER(7),PERIM)
0020 DATA VOLHIS/80*0./,FREHIS/80*0./
0021 DATA NOZOD /'N','O','Z','Z','L','E',' ','I','D',' ',' ',' ',' '/
    C
    C Open data file
0022 451  FORMAT(0,22A1)
0023 TYPE *, ' Enter filename'
0024 ACCEPT 451,LONGO,(FILENAME(I),I=1,LONGO)
    C
0025 OPEN(UNIT=3,NAME=FILENAME,TYPE='OLD',
0026 10ISP='KEEP',ACCESS='DIRECT',RECORDSIZE=4,FORM='UNFORMATTED')
0027 READ(3*1) IBUFER
0028 NUHE=IBUFER(1)
0029 ICNT=0
0030 SHD4=0.
0031 SHD3=0.
0032 SHD2=0.
0033 DTOT=0.
0034 ESTOT=0.
0035 PI=3.14159
0036 Q1=4./(3.*SORT(PI))
    C
    C Main loop
0037 DO 100 K=2,NUHE
0038 READ(3*K) IBUFER
0039 IF (IBUFER(1).EQ.0) GO TO 200
0040 ICNT=ICNT+1
0041 D2=(4.*AREA)/PI
0042 D=SOR(T(D2))
0043 D3=D2*D
0044 D4=D2*D2
0045 ESFER(ICNT)=(PERIM*PERIM)/(AREA*4.*PI)
    DBUF(ICNT)=D
  
```

```
0046      VOBUF(icont)=Q1*(AREA**1.5)
0047      SHD4=SHD4+D4
0048      SHD3=SHD3+D3
0049      SHD2=SHD2+D2
0050      DTOT=DTOT+D
0051      ESTOT=ESTOT+ESFER(icont)
0052      II=1.9*D
0053      II=MINI(79,II)
0054      FREHIS(II)=FREHIS(II)+1
0055      VOLHIS(II)=VOLHIS(II)+D3
0056      100  CONTINUE
0057      CLOSE(UNIT=3)
0058      GO TO 300
0059      200  CLOSE(UNIT=3)
0060      TYPE *, ' File records counter error'
0061      CALL EXIT
C
C          Begin general statistic
C
0062      300  TYPE *, ' Enter nozzle code'
0063      ACCEPT 750, ITEX, (NOZIN(I), I=1, ITEX)
0064      750  FORMAT(Q,68A1)
0065      TYPE *, ' Enter water pressure (psi)'
0066      ACCEPT *, WATP
0067      TYPE *, ' Enter wind tunnel speed (ft/sec)'
0068      ACCEPT *, WTS
0069      TYPE *, ' Enter downstream coordinate (inch)'
0070      ACCEPT *, DOWL
0071      PRINT 4, NOZOD, (NOZIN(I), I=1, ITEX)
0072      PRINT 5, WATP
0073      PRINT 6, WTS
0074      PRINT 7, DOWL
0075      PRINT 11, ICONT
0076      4    FORMAT(X,12A1,68A1)
0077      5    FORMAT(' Water pressure =', F6.2, ' psi')
0078      6    FORMAT(' Wind tunnel speed =', F6.2, ' ft/sec')
0079      7    FORMAT(' Downstream location =', F6.2, ' inch')
0080      11   FORMAT(' Number of Drops =', I5)
0081      PRINT 12
0082      FORMAT(' Length diameter (D18) ')
0083      NAMO=ICONT
0084      CALL STATS(NAMO,DBUF,DTOT)
0085      PRINT 13, SQRT(SMD2/FLOAT(ICONT))
0086      13   FORMAT(' Area mean diameter (D20)=', F15.6)
0087      COMOD=SMD3*PI/6.
0088      PRINT 17, COMOD
0089      17   FORMAT(' Drops total volume=', F15.6)
0090      NAMO=ICONT
0091      CALL STATS(NAMO, VOBUF, COMOD)
0092      VOLMED=SMD3/FLOAT(ICONT)
0093      VOLMED=VOLMED**(.1./3.)
0094      PRINT 14, VOLMED
0095      14   FORMAT(' Volume mean diameter (D30)=', F15.6)
0096      PRINT 16, SMD3/SMD2
0097      16   FORMAT(' Sauter mean diameter (D32)=', F15.6)
0098      PRINT 30, SHD4/SMD3
```

ORIGINAL PAGE IS
OF POOR QUALITY

```

FORTRAN IV-P          V02-51          18:58:30      23-FEB-84      P   3
RAINST.FTN           /TR:BLOCKS/WR

0100      30      FORMAT(' Volume distribution mean diameter (D43)=',F15.6)
0101      PRINT 31
0102      FORMAT(' Circularity (perimeter**2/area*4pi)')
NAMO=ICONT
0103      CALL STATS(NAMO,ESFER,ESTOT)
0104      TYPE *, ' Plot the distributions (Y/N)'
ACCEPT 800,ANSA
0105      FORMAT(A1)
0106      808      IF (ANSA.NE.'Y') GO TO 800
0107      OPEPLO=0
0108      SAMP=FLOAT(ICONT)/100.
0109      SHD3=SHD3/100.
0110      DO 500 K=8,79
0111      VOLHIS(K)=VOLHIS(K)/SHD3
0112      FREHIS(K)=FREHIS(K)/SAMP
0113      CONTINUE
0114      500      TYPE *, ' Frequency distribution (Y/N)'
ACCEPT 800,ANSA
0115      IF (ANSA.NE.'Y') GO TO 600
0116      CALL RAINHIK(FREHIS,OPEPLO,0,.,1)
0117      IF (OPEPLO.EQ.0) GO TO 600
0118      OPEPLO=-OPEPLO
0119      CALL SYMBOL(-4.3,1,15,.,1,'DROPS DIAMETER FREQUENCY DISTRIBUTION',
1         00,137)
0120      CALL SYMBOL(-1.35,-.75,.,1,'FREQUENCY (%)',100.,13)
0121      GO TO 480
0122      600      TYPE *, ' Cumulative volume distribution (Y/N)'
ACCEPT 800,ANSA
0123      IF (ANSA.NE.'Y') GO TO 650
0124      CALL RAINHIK(VOLHIS,OPEPLO,0,.,1)
0125      IF (OPEPLO.GE.0) GO TO 650
0126      CALL SYMBOL(-4.3,1,45,.,1,'VOLUME CONTRIBUTION VS DIAMETER',90.,31)
0127      CALL SYMBOL(-.05,-.75,.,1,'VOLUME CONTRIBUTION (%)',100.,23)
0128      CALL SYMBOL(.7,2,35,.,1,'DIAMETER (MM)',90.,13)
0129      CALL SYMBOL(-5.5,0,.,1,NOZID,90.,1TEX+12)
0130      CALL SYMBOL(-5.25,2.25,.,1,WATP,90.,-1)
0131      480      CALL SYMBOL(-5.0,0,.,1,WATP,90.,-1)
0132      CALL NUMBER(-5.25,2.25,.,1,WATP,90.,-1)
0133      CALL SYMBOL(-5.0,0,.,1,'WIND TUNNEL SPEED (FT/SEC)',90.,26)
0134      CALL NUMBER(-5.0,2.05,.,1,WTS,90.,-1)
0135      CALL SYMBOL(-4.75,0,.,1,'DOWNSTREAM STATION (INCH)',90.,25)
0136      CALL NUMBER(-4.75,2.75,.,1,DOWL,90.,-1)
0137      IF (OPEPLO.GT.0) GO TO 600
0138      650      IF (OPEPLO.NE.0) CALL PLOT(0.,0.,999)
0139      600      CALL EXIT
0140      END

```

APPENDIX C
DROPLET DATA

DROPLET DATA FOR NEGATIVE 1

Droplet No.	Diameter (mm)						
1	0.5243418	36	1.18004	71	0.6642479	106	0.2157810
2	0.1561709	37	0.1412618	72	0.3766983	107	1.201418
3	0.1631151	38	0.2864208	73	1.752381	108	0.4589501
4	0.2258227	39	0.6317422	74	0.1631151	109	0.3296110
5	0.5670060	40	0.1245812	75	0.1697756	110	1.016475
6	0.1489031	41	0.3395512	76	0.5993233	111	0.1153398
7	0.2745637	42	0.5179601	77	0.2157810	112	0.2940600
8	0.3939605	43	0.6387230	78	0.5591305	113	0.4565282
9	0.1331829	44	0.8436380	79	0.9661503	114	0.2785721
10	0.4685126	45	0.6103209	80	0.6211239	115	0.4211615
11	0.5937480	46	0.5766991	81	0.3262303	116	1.182819
12	0.1883491	47	0.7794333	82	0.1331829	117	1.805354
13	0.4613593	48	0.7949249	83	0.7094414	118	0.7460029
14	0.6524605	49	0.1631151	84	0.2535728	119	0.9865882
15	0.2354364	50	0.5571443	85	0.2446727	120	0.8317273
16	0.1489031	51	0.1883491	86	0.6774681	121	1.021913
17	0.1245812	52	0.4755583	87	0.2621709	122	0.1331829
18	0.3707657	53	0.1631151	88	0.1823683	123	0.1412618
19	0.1245812	54	0.5222232	89	0.6936390	124	1.678713
20	0.4893454	55	0.9832113	90	0.1489031	125	0.4825011
21	0.3193615	56	0.3967645	91	0.1489031	126	0.5689578
22	0.1697756	57	0.4661403	92	0.2825237	127	0.1153398
23	0.1489031	58	0.7935290	93	0.5551509	128	0.1761845
24	0.1245812	59	0.5093269	94	0.4050601	129	0.2306796
25	0.1489031	60	0.1489031	95	0.7548665	130	0.4589501
26	0.8656892	61	0.1489031	96	0.5591305	131	0.6524605
27	0.2663659	62	0.2902655	97	0.2535728	132	0.3123417
28	0.7047380	63	0.2825237	98	0.3087720	133	0.2400990
29	0.1561709	64	0.2902655	99	0.1153398	134	0.1941458
30	0.6904351	65	0.4637560	100	0.3228141	135	1.315076
31	0.1823683	66	0.3492087	101	0.6121347	136	0.1245812
32	1.167727	67	1.727532	102	0.1761845	137	0.4732214
33	0.1823683	68	0.1561709	103	0.4131892	138	0.3395512
34	0.1941458	69	1.462741	104	0.6387230	139	0.7264272
35	0.4104974	70	0.1561709	105	0.3967645	140	0.4237855

DROPLET DATA FOR NEGATIVE 1 (cont'd)

Droplet No.	Diameter (mm)						
176	0.1941458	211	0.3296110	246	0.1823683		
177	0.9684424	212	1.373626	247	1.751115		
178	0.4565282	213	0.3825389	248	0.5805310		
179	0.6507592	214	0.8087506	249	0.1489031		
180	0.4960953	215	0.1153398	250	0.2157810		
181	0.5900019	216	0.6642479	251	0.2704958		
182	0.4708728	217	1.852632	252	0.6575381		
183	0.2258227	218	0.1761845	253	0.1412618		
184	0.3262303	219	0.5264518	254	0.1245812		
185	1.063381	220	0.2825237	255	0.3939605		
186	0.1941458	221	0.5786182	256	0.2902655		
187	1.131075	222	0.2864208	257	0.3647365		
188	0.2579077	223	0.3123417	258	0.4315621		
189	0.1561709	224	0.5430371	259	0.5049549		
190	0.5027546	225	0.1823683	260	0.6103209		
191	0.5786182	226	0.5071455	261	0.1412618		
192	0.6541575	227	0.3296110	262	0.7822727		
193	0.3262303	228	0.3616843	263	1.276578		
194	1.575138	229	0.5591305	264	0.2354364		
195	0.1245812	230	0.1331829	265	0.7031631		
196	0.5571443	231	0.4825011	266	0.8410058		
197	0.2354364	232	0.1941458	267	0.5450747		
198	0.5974706	233	0.2306796				
199	1.077877	234	0.5551509				
200	0.3555012	235	0.3428006				
201	0.2258227	236	0.1412618				
202	0.4467092	237	0.1331829				
203	2.063262	238	0.7233686				
204	0.2785721	239	0.5709030				
205	0.3825389	240	0.2400990				
206	2.363294	241	0.1697756				
207	0.3586060	242	0.2208589				
208	0.4801979	243	0.5264518				
209	1.219733	244	0.2208589				
210	0.4516453	245	0.5974706				

DROPLET DATA FOR NEGATIVE 2

Droplet No.	Diameter (mm)								
1	0.1331829	36	0.8488781	71	0.4392009	106	0.4755583	141	0.3123417
2	0.7533965	37	0.6952354	72	0.3586060	107	1.302370	142	1.726248
3	0.6984173	38	0.6121347	73	0.4847932	108	0.3329574	143	0.9752867
4	0.4516453	39	0.1761845	74	0.1153398	109	0.1561709	144	2.713552
5	0.2864208	40	1.190294	75	0.4938556	110	0.1823683	145	0.4211615
6	0.4847932	41	1.405538	76	0.3395512	111	0.9008328	146	0.6807330
7	0.4801979	42	0.3193615	77	0.2105807	112	1.164875	147	0.1245812
8	0.4392009	43	1.278314	78	0.3523690	113	0.5531504	148	0.2208589
9	0.6456283	44	0.1561709	79	0.5093269	114	0.2354364	149	0.2208589
10	0.2745637	45	0.5114988	80	0.2306796	115	1.724963	150	0.2105807
11	0.1489031	46	0.3123417	81	0.3737437	116	0.8566780	151	1.266114
12	0.7665254	47	0.7294731	82	1.057107	117	1.191225	152	1.673421
13	0.7015847	48	0.7294731	83	0.3737437	118	0.8656892	153	1.363907
14	0.5264518	49	0.7822727	84	0.7294731	119	0.2940600	154	1.805968
15	0.1697756	50	0.8896880	85	0.6456283	120	0.3296110	155	0.1489031
16	0.2785721	51	1.473313	86	0.8462621	121	0.3296110	156	0.7851019
17	0.1883491	52	0.9638526	87	0.5805310	122	0.4613593	157	0.1997744
18	0.2704958	53	0.5049549	88	0.1941458	123	0.3939605	158	0.4237855
19	0.7309912	54	0.8290572	89	0.3296110	124	0.2902655	159	0.3492087
20	0.2491625	55	0.3586060	90	0.5049549	125	0.1331829	160	0.7865127
21	0.1997744	56	1.278314	91	0.2535728	126	0.2052487	161	1.122219
22	0.3939605	57	0.3428006	92	0.2208589	127	0.9546068	162	0.2535728
23	0.2978061	58	0.5179601	93	0.4540933	128	1.173409	163	0.1561709
24	0.2306796	59	1.052904	94	0.5918780	129	0.2579077	164	0.6473432
25	0.5368776	60	1.296398	95	0.5862319	130	0.6575381	165	0.7694125
26	0.1245812	61	0.1245812	96	0.4289856	131	1.224269	166	0.1631151
27	0.1561709	62	1.161062	97	0.3193615	132	0.5551509	167	0.1489031
28	0.1245812	63	0.9592409	98	0.6659148	133	0.1631151	168	0.4211615
29	0.4613593	64	1.345906	99	0.2306796	134	2.012671	169	0.3193615
30	0.8859419	65	1.190294	100	0.6030114	135	0.5430371	170	0.6175439
31	0.4983250	66	0.8169339	101	0.3766983	136	0.2745637	171	0.1331829
32	0.8317273	67	1.261728	102	0.1331829	137	0.9008328	172	0.3586060
33	0.8707965	68	0.2446727	103	0.2621709	138	0.2306796	173	1.098255
34	0.1561709	69	0.4050601	104	0.9251183	139	1.197721	174	0.6282227
35	0.9752867	70	0.4825011	105	0.1761845	140	0.3460194	175	1.071688

ORIGINAL PAGE IS
OF POOR QUALITY

DROPLET DATA FOR NEGATIVE 2 (cont'd)

Droplet No.	Diameter (mm)						
176	1.120242						
177	0.2258227						
178	0.8644077						
179	0.1245812						
180	0.2052487						
181	1.320964						
182	0.2157810						
183	0.6839823						
184	0.1331829						
185	0.1331829						
186	0.2052487						
187	0.3825389						
188	0.1941453						
189	0.3492087						
190	0.1412618						
191	0.3796298						
192	0.2704958						
193	0.4661403						
194	0.2978061						
195	0.2400990						
196	0.4938556						
197	1.672096						
198	0.2400990						
199	0.1153398						
200	0.3395512						
201	0.5071455						
202	0.4847932						
203	0.3586060						
204	1.110302						
205	0.1883491						
206	0.6352422						
207	0.2579077						

DROPLET DATA FOR NEGATIVE 3

Droplet No.	Diameter (mm)								
1	0.2052487	36	0.4916057	71	0.3854260	106	0.4315621	141	0.4870746
2	0.5709030	37	0.1631151	72	0.1883491	107	0.1631151	142	0.3911363
3	0.1561709	38	0.3882917	73	0.4104974	108	0.2105807	143	1.618871
4	0.7294731	39	0.5158154	74	0.2400990	109	0.9650021	144	0.4392009
5	0.3329574	40	0.2579077	75	0.3158711	110	0.4315621	145	0.2306796
6	0.1245812	41	0.2354364	76	0.1331829	111	0.1697756	146	0.4589501
7	0.3882917	42	0.1561709	77	0.2208589	112	0.1245812	147	0.8114876
8	0.4050601	43	0.5136616	78	0.8087506	113	1.204183	148	0.2745637
9	0.5071455	44	0.2208589	79	0.3296110	114	1.467281	149	0.2052487
10	0.2446727	45	0.2940600	80	1.197721	115	0.1761845	150	0.3262303
11	0.1153398	46	0.1245812	81	0.2105807	116	0.1331829	151	0.1631151
12	0.1997744	47	0.5264518	82	0.3882917	117	0.6011702	152	0.3051605
13	0.9322807	48	0.1631151	83	0.4050601	118	0.2400990	153	0.1761845
14	1.322641	49	0.2258227	84	0.1823683	119	3.194656	154	0.7094414
15	0.2902655	50	0.9298993	85	0.2491625	120	1.217914	155	0.7125599
16	0.4392009	51	0.1489031	86	0.2258227	121	0.2745637	156	0.4392009
17	0.1245812	52	0.4916057	87	0.4870746	122	0.5862319	157	0.1561709
18	0.1331829	53	0.1697756	88	0.3647365	123	0.2825237	158	0.3939605
19	0.3123417	54	0.2663659	89	0.1997744	124	0.2258227	159	0.5900019
20	0.3015057	55	0.6609015	90	0.1631151	125	0.2157810	160	0.1331829
21	0.6609015	56	0.7851019	91	0.1997744	126	0.3911363	161	0.9405677
22	0.1489031	57	0.7519236	92	0.3362705	127	1.526529	162	0.1697756
23	0.6524605	58	0.2940600	93	0.7990977	128	0.3523690	163	0.6642479
24	0.2052487	59	1.053956	94	0.2491625	129	1.961342	164	1.213354
25	0.6229062	60	0.4491840	95	0.3677634	130	1.411834	165	0.6592219
26	0.5114988	61	0.7650778	96	0.6888276	131	0.4732214	166	1.418883
27	0.1245812	62	0.3395512	97	1.017565	132	0.4637560	167	0.1331829
28	0.1941458	63	0.4237855	98	0.1697756	133	0.2354364	168	0.6741873
29	0.6524605	64	1.192155	99	0.2105807	134	2.418930	169	0.7851019
30	0.3362705	65	0.3677634	100	0.4131892	135	1.812096	170	0.2491625
31	0.3228141	66	0.2825237	101	0.1412618	136	0.1153398	171	0.1153398
32	0.3796298	67	2.182332	102	2.134566	137	0.1153398	172	0.6968281
33	0.2785721	68	1.173409	103	0.2208589	138	0.4825011	173	0.6264555
34	0.6334946	69	0.2785721	104	1.887607	139	0.1561709	174	0.8449511
35	0.9370251	70	0.3647365	105	0.5571443	140	0.2052487	175	1.965295

DROPLET DATA FOR NEGATIVE 3 (cont'd)

Droplet No.	Diameter (mm)						
176	0.2446727	211	0.7607183	246	0.2157810		
177	0.9695865	212	0.2902655	247	0.5650474		
178	0.1697756	213	0.6439089	248	0.5179601		
179	0.2208589	214	0.9730106	249	0.1245812		
180	0.2663659	215	0.4237855	250	0.7708520		
181	1.068581	216	0.1997744	251	0.5264518		
182	0.7340181	217	0.3262303	252	0.8884411		
183	0.5956123	218	0.4637560	253	0.2306796		
184	0.1245812	219	0.1331829	254	0.3123417		
185	0.5285534	220	0.1697756	255	0.9684424		
186	0.4755583	221	0.2052487	256	0.1997744		
187	0.2621709	222	0.1412618				
188	0.2864208	223	0.7935290				
189	0.1697756	224	0.2745637				
190	0.1331829	225	0.5974706				
191	0.7340181	226	0.3707657				
192	0.8236910	227	0.4708728				
193	0.4131892	228	0.6936390				
194	0.1331829	229	0.1883491				
195	0.3796298	230	0.3677634				
196	0.1245812	231	0.8182897				
197	1.225175	232	0.5862319				
198	0.3586060	233	0.2663659				
199	0.1631151	234	0.6299849				
200	0.1697756	235	0.3586060				
201	0.1153398	236	0.1489031				
202	0.1941458	237	0.9130563				
203	0.1331829	238	0.2258227				
204	0.5805310	239	0.5005447				
205	1.020828	240	0.7031631				
206	1.968113	241	0.4185209				
207	0.1761845	242	0.5114988				
208	0.1561709	243	0.2621709				
209	1.074787	244	0.9775574				
210	0.1412618	245	0.8410058				

DROPLET DATA FOR NEGATIVE 4

Droplet No.	Diameter (mm)								
1	0.5709030	36	0.9499502	71	0.7636274	106	0.2208589	141	0.6456283
2	0.8707965	37	0.6558500	72	0.3228141	107	0.6524605	142	0.4366695
3	0.3707657	38	2.033495	73	0.2579077	108	1.117269	143	0.2400990
4	0.3766983	39	0.9603959	74	0.1245812	109	0.1331829	144	0.1697756
5	0.5766991	40	0.2354364	75	0.4366695	110	0.1412618	145	0.4211615
6	0.1561709	41	0.7765834	76	0.5071455	111	0.1489031	146	0.4050601
7	0.2978061	42	0.4185209	77	0.3329574	112	0.6103209	147	0.5179601
8	0.1697756	43	0.9166915	78	0.5136616	113	0.4185209	148	0.1561709
9	0.2157810	44	0.3707657	79	1.669442	114	0.8644077	149	0.2105807
10	0.5747736	45	0.5918780	80	0.6317422	115	1.376850	150	0.8032488
11	1.0044046	46	1.460465	81	0.3015057	116	0.2446727	151	0.6369849
12	0.2052487	47	0.7694125	82	1.760586	117	0.3737437	152	0.1883491
13	0.4315621	48	0.4778837	83	1.650743	118	0.7141140	153	0.1631151
14	0.3586060	49	0.1761845	84	0.8707965	119	0.8746075	154	0.1631151
15	0.9944228	50	0.5327318	85	1.136941	120	0.6473432	155	0.4211615
16	0.3523690	51	0.3939605	86	0.2785721	121	1.266989		
17	0.2354364	52	0.6246834	87	0.8317273	122	0.5049549		
18	0.9786908	53	0.9057420	88	1.728174	123	0.2940600		
19	0.7851019	54	0.3460194	89	2.441738	124	0.6659148		
20	0.2579077	55	0.4131892	90	0.8004838	125	1.347552		
21	0.3087720	56	0.3616843	91	0.6085018	126	0.5049549		
22	0.3677634	57	0.5005447	92	0.5650474	127	0.2052487		
23	0.1153393	58	0.2157810	93	0.1489031	128	0.3428006		
24	1.345082	59	0.1331829	94	0.1631151	129	0.1245812		
25	0.6725409	60	0.7355269	95	0.5491273	130	0.8370419		
26	0.3329574	61	0.7577981	96	0.1245812	131	0.2258227		
27	1.1022835	62	0.4131892	97	0.1997744	132	0.2400990		
28	0.2157810	63	0.2208589	98	0.2258227	133	0.5709030		
29	1.245812	64	0.1631151	99	0.1823683	134	0.8846897		
30	1.881725	65	0.5670060	100	0.1883491	135	0.1153398		
31	0.3911363	66	0.6741873	101	1.226983	136	0.2491625		
32	1.237778	67	0.8983681	102	0.3158711	137	0.6421849		
33	0.1761845	68	0.7415313	103	0.8018675	138	0.3492087		
34	1.422005	69	0.6473432	104	0.4516453	139	0.4613593		
35	0.3995488	70	0.1761845	105	0.5900019	140	0.3051605		

DROPLET DATA FOR NEGATIVE 5

ORIGINAL PAGE IS
OF POOR QUALITY

Droplet No.	Diameter (mm)								
1	0.5348087	36	1.156278	71	1.072722	106	0.2446727	142	0.3015057
2	0.2825237	37	2.265579	72	0.3362705	107	0.8223441	143	0.4613593
3	0.1489031	38	0.8771389	73	0.2621709	108	0.5843378	144	0.5591305
4	0.4237855	39	0.8784019	74	1.262607	109	0.3825389	145	0.4104974
5	0.4211615	40	0.1631151	75	0.3296110	110	0.4960953	146	1.127148
6	0.2535728	41	0.1697756	76	0.1823683	111	0.1489031	147	1.3475532
7	0.2978061	42	0.7665254	77	0.1412618	112	0.4755583	148	0.1153398
8	0.4825011	43	0.2157810	78	0.4847932	113	0.9106247	149	0.2785721
9	0.2940600	44	0.3939605	79	0.1761845	114	6.326891	150	0.4366695
10	0.1245812	45	1.881725	80	0.7279517	115	0.4516453	151	0.1697756
11	0.7548665	46	0.4289856	81	1.188429	116	0.2579077	152	0.5862319
12	0.1761845	47	1.646709	82	1.027323	117	0.3228141	153	0.3228141
13	0.8169339	48	0.3228141	83	0.6175439	118	1.006611	154	0.2825237
14	0.1997744	49	0.9999814	84	1.994412	119	0.2864208	155	0.3523690
15	0.1697756	50	1.391268	85	0.8357164	120	1.354936	156	0.2306796
16	0.5285534	51	0.7325062	86	0.1489031	121	0.1489031	157	1.028402
17	0.4366695	52	0.1331829	87	0.4211615	122	0.3362705	158	0.1331829
18	0.9557675	53	0.3911363	88	3.548145	123	2.172148	159	0.2621709
19	0.9843382	54	0.1631151	89	1.033778	124	0.9429221	160	0.4870746
20	0.5179601	55	0.7294731	90	0.1331829	125	1.215180	161	0.2306796
21	0.5243418	56	1.098255	91	0.5611097	126	0.4315621	162	0.2663659
22	0.7679704	57	0.2902655	92	0.2446727	127	0.3555012	163	0.3555012
23	0.1823683	58	0.5409917	93	0.2535728	128	0.5430371	164	0.8357164
24	0.6456283	59	0.2940600	94	0.65556500	129	0.6352422	165	0.7708520
25	0.9382074	60	0.6030114	95	0.6952354	130	0.2208589	166	0.4847932
26	0.57666991	61	0.2306796	96	2.299094	131	0.7794333	167	0.5114988
27	0.7172121	62	0.2354364	97	0.1412618	132	1.495716	168	0.3460194
28	0.1997744	63	0.5993233	98	0.1489031	133	0.2258227	169	0.7694125
29	0.7430249	64	1.044446	99	0.1331829	134	0.5918780	170	0.1153398
30	2.168061	65	0.1331829	100	0.3158711	135	0.1153398	171	0.1697756
31	0.4825011	66	0.2400990	101	0.2208589	136	0.5285534	172	0.2825237
32	1.548162	67	0.7325062	102	0.4801979	137	0.2400990	173	0.5591305
33	1.087094	68	0.3616843	103	0.3737437	138	0.5306467	174	0.2105807
34	1.122219	69	0.6066772	104	0.6369849	139	0.4263935	175	0.1412618
35	1.032705	70	0.2306796	105	0.5491273	140	0.8605515	176	0.6246834
								177	0.4637560
								178	0.3296110
								179	0.9786908

DROPLET DATA FOR NEGATIVE 6

Droplet No.	Diameter (mm)						
1	0.3395512	36	0.4732214	71	0.5200961	106	0.2258227
2	0.6299849	37	0.6904351	72	0.4366695	107	0.4185209
3	0.2354364	38	0.5368776	73	0.1489031	108	0.2258227
4	0.4185209	39	0.4104974	74	0.6524605	109	0.1489031
5	0.6439089	40	0.8004838	75	1.357388	110	0.5027546
6	0.3523690	41	0.6872163	76	0.1245812	111	0.8087506
7	0.4565282	42	0.4685126	77	0.4237855	112	2.016524
8	0.1489031	43	0.1331829	78	0.2354364	113	0.2105807
9	0.5974706	44	0.7963182	79	0.2704958	114	0.4104974
10	0.4341233	45	0.6246834	80	0.6404563	115	0.3015057
11	0.3395512	46	0.2400990	81	0.2745637	116	1.681352
12	0.5786182	47	0.3586060	82	0.7031631	117	2.049785
13	0.1245812	48	1.109303	83	0.6317422	118	0.1153398
14	0.4131892	49	0.4613593	84	0.1412618	119	0.5747736
15	0.3193615	50	0.3492087	85	0.6968281	120	0.9534448
16	0.2208589	51	0.9627018	86	0.6085018	121	0.4104974
17	0.4158636	52	0.3707657	87	0.8330591	122	0.4613593
18	0.4417179	53	0.2978061	88	0.4050601	123	0.2579077
19	0.2940600	54	0.2940600	89	0.3939605	124	1.502372
20	0.6791024	55	0.3586060	90	0.2864208	125	0.4708728
21	0.1412618	56	0.6473432	91	1.097245	126	0.1412618
22	0.1883491	57	0.3555012	92	1.731378	127	0.1153398
23	0.3228141	58	1.387278	93	2.829158	128	0.3555012
24	0.2306796	59	0.2354364	94	0.4467092	129	2.176737
25	0.2902655	60	0.9008328	95	0.7607183	130	1.996079
26	0.3911363	61	0.6541575	96	0.1823683	131	0.5136616
27	0.2306796	62	0.3123417	97	0.3911363	132	0.3967645
28	0.6421849	63	0.2902655	98	0.8032488	133	0.4938556
29	0.3158711	64	0.3677634	99	0.1697756	134	0.3193615
30	0.5409917	65	0.9865882	100	0.5881200	135	1.280913
31	0.4732214	66	1.689246	101	0.1245812	136	1.041257
32	0.4417179	67	0.6030114	102	0.1245812	137	1.163923
33	0.9346558	68	0.1331829	103	0.2306796	138	0.4893454
34	0.53889386	69	0.1153398	104	0.2446727	139	0.5285534
35	0.5179601	70	0.4392009	105	0.9358413	140	0.2978061

DROPLET DATA FOR NEGATIVE 6 (cont'd)

Droplet No.	Diameter (mm)						
176	0.1489031						
177	0.4289856						
178	0.6952354						
179	0.1697756						
180	0.4613593						
181	0.4870746						
182	1.185627						
183	0.4185209						
184	0.2785721						
185	0.4613593						
186	0.6439089						
187	0.5348087						
188	0.2785721						
189	0.2621709						
190	0.4050601						
191	0.6264555						
192	0.8859419						
193	0.2491625						
194	0.8527870						
195	0.1997744						
196	0.1761845						
197	0.1412618						
198	0.6334946						
199	0.62229062						
200	0.3647365						
201	0.3460194						
202	0.1941458						
203	0.3523690						
204	0.6066772						
205	0.5824375						
206	0.3395512						
207	0.1489031						
208	0.5843378						
209	0.3395512						
210	0.1761845						
211	0.1823683						
212	0.3262303						

DROPLET DATA FOR NEGATIVE 7

Droplet No.	Diameter (mm)						
1	0.6558500	36	0.3087720	71	0.6952354	106	0.3087720
2	0.1331829	37	1.098255	72	0.2446727	107	0.6541575
3	0.4366695	38	0.3677634	73	0.6282227	108	0.2579077
4	0.2208589	39	1.165826	74	1.206942	109	1.068581
5	0.4263935	40	0.1761845	75	0.1245812	110	1.762474
6	0.1489031	41	0.3523690	76	0.2785721	111	0.2621709
7	0.7607183	42	0.9615495	77	0.5071455	112	0.5027546
8	0.8475711	43	0.3492087	78	0.3051605	113	0.3051605
9	0.2491625	44	0.3616843	79	0.2208589	114	0.5049549
10	0.3616843	45	0.2902655	80	0.6659148	115	1.515596
11	0.1153398	46	0.3766983	81	0.5306467	116	0.1823683
12	0.2940600	47	0.6659148	82	0.3329574	117	0.4467092
13	0.8004838	48	0.1245812	83	1.243140	118	0.9672971
14	1.097245	49	0.6157461	84	0.1697756	119	0.9921906
15	0.1245812	50	0.8196434	85	0.1489031	120	0.7751545
16	0.1412618	51	0.4778837	86	0.3051605	121	1.159151
17	0.1631151	52	0.3296110	87	0.1697756	122	0.1245812
18	0.1245812	53	0.5471048	88	1.733298	123	1.106301
19	0.2621709	54	0.3262303	89	0.8209949	124	0.2052487
20	0.4708728	55	1.220642	90	0.4685126	125	0.1153398
21	0.5591305	56	0.1245812	91	0.1941458	126	1.738407
22	0.4916057	57	0.3586060	92	0.4263935	127	0.3228141
23	0.3329574	58	0.1883491	93	0.3616843	128	2.043827
24	0.1153398	59	0.6592219	94	0.4893454	129	1.695142
25	0.3158711	60	0.9592409	95	0.5993233	130	2.414802
26	0.1997744	61	0.2105807	96	0.1489031	131	0.9820831
27	0.6193365	62	0.8644077	97	0.4685126	132	1.233291
28	0.5158154	63	0.2105807	98	0.4077878	133	2.761740
29	0.3995488	64	0.6490534	99	0.3087720	134	0.1412618
30	0.7836886	65	1.463498	100	0.1761845	135	0.2491625
31	0.4077878	66	0.3051605	101	0.2785721	136	0.3051605
32	0.4801979	67	0.4565282	102	0.5709030	137	0.2446727
33	0.4077878	68	0.2052487	103	0.8983681	138	0.4023139
34	0.9142697	69	1.272228	104	0.4708728	139	1.986615
35	0.2400990	70	0.2940600	105	0.2052487	140	0.4589501

ORIGINAL PAGE
OF POOR QUALITY

DROPLET DATA FOR NEGATIVE 7 (cont'd)

Droplet No.	Diameter (mm)						
176	0.7047380	211	0.1489031				
177	0.2535728	212	0.5049549				
178	1.665453	213	0.7047380				
179	1.950573	214	0.4442205				
180	0.1489031	215	0.2208589				
181	0.3262368	216	0.3492087				
182	1.212440	217	0.1631151				
183	0.4023139	218	0.2902655				
184	1.044446	219	0.5591305				
185	0.5285534	220	1.570204				
186	0.8250359	221	0.3193615				
187	0.2535728	222	0.3123417				
188	0.3428006	223	0.3193615				
189	0.1697756	224	0.2258227				
190	0.7218344	225	0.2663659				
191	0.3766983	226	1.280047				
192	0.2704958	227	0.1153398				
193	0.8758741	228	0.3995488				
194	0.8082506	229	1.194941				
195	0.1489031	230	1.175297				
196	1.123207	231	0.4211615				
197	0.4516453	232	0.7000028				
198	0.7460029	233	0.2940600				
199	0.2105807	234	0.3737437				
200	0.4825011	235	0.2157810				
201	0.2579077	236	0.2306796				
202	0.8317273	237	0.6856012				
203	0.5348067	238	0.4341233				
204	1.044446	239	0.2157810				
205	1.444436	240	0.7031631				
206	0.2208589	241	0.6507592				
207	0.5974706	242	0.4392009				
208	0.4263935	243	0.3882917				
209	1.573025						
210	0.4825011						

ORIGINAL PAGE IS
OF POOR QUALITY

DROPLET DATA FOR NEGATIVE 8

Droplet No.	Diameter (mm)						
1	0.1331829	36	0.1823683	71	0.5114988	106	0.7504478
2	0.4708728	37	0.5471048	72	0.8656892	107	0.4847932
3	0.1489031	38	0.3854260	73	0.7340181	108	1.024081
4	0.4417179	39	0.7694125	74	0.5049549	109	0.3882917
5	0.8223441	40	0.2105807	75	0.7722889	110	0.2491625
6	0.3051605	41	0.2306796	76	0.5611097	111	0.1697756
7	0.8018675	42	1.240462	77	0.1883491	112	0.1631151
8	0.3616843	43	0.2704958	78	0.2354364	113	0.1331829
9	0.4158636	44	0.2621709	79	0.5327318	114	0.1941458
10	0.3707657	45	0.1331829	80	0.9429221	115	0.2621709
11	0.3647365	46	0.5005447	81	0.7279517	116	0.1245812
12	0.1941458	47	0.6139430	82	0.5158154	117	0.6404563
13	0.3766983	48	0.1412618	83	0.3087720	118	0.3123417
14	1.212440	49	0.2354364	84	0.5993233	119	0.9854638
15	0.6011702	50	0.6193365	85	0.9933073	120	0.2663659
16	0.7780096	51	0.3707657	86	1.601660	121	0.3158711
17	0.2940600	52	0.6575381	87	0.5747736	122	0.2579077
18	0.4661403	53	0.2400990	88	0.5471048	123	0.1245812
19	0.2052487	54	0.1489031	89	0.1561709	124	0.7385352
20	0.3616843	55	0.5531504	90	0.3825389	125	0.4755583
21	0.8330591	56	1.055007	91	0.2491625	126	0.3395512
22	1.519979	57	0.2208589	92	0.3854260	127	0.3296110
23	0.2157810	58	0.8946584	93	0.4077878	128	0.6558500
24	0.1631151	59	0.5306467	94	0.2621709		
25	0.2978061	60	0.3228141	95	0.7031631		
26	0.5843378	61	0.2052487	96	0.9499502		
27	0.3193615	62	0.4467092	97	0.2208589		
28	0.7078770	63	0.2446727	98	0.4491640		
29	1.204183	64	0.6264555	99	0.9534448		
30	0.2621709	65	0.4341233	100	0.2446727		
31	0.2825237	66	0.4847932	101	0.5728415		
32	1.287818	67	1.195869	102	0.2208589		
33	1.035920	68	1.091166	103	0.1997744		
34	0.4685126	69	1.064423	104	0.2400990		
35	0.8540859	70	0.2258227	105	0.3051605		

ORIGINAL PAGE IS
OF POOR QUALITY

DROPLET DATA FOR NEGATIVE 9

Droplet No.	Diameter (mm)								
1	0.3796298	36	0.2940600	71	0.3616843	106	0.6282227	141	0.1331829
2	0.3428006	37	0.1331829	72	0.1245812	107	0.2400990	142	0.1331829
3	0.2785721	38	0.5005447	73	0.3460194	108	0.3460194	143	0.7907299
4	0.4417179	39	0.8032488	74	0.6085018	109	1.058155	144	1.16277
5	0.2621709	40	0.8669688	75	0.4417179	110	0.5843378	145	0.1631151
6	0.2535729	41	0.8475711	76	0.6387230	111	0.3158711	146	1.060248
7	0.1153398	42	0.4755583	77	0.1631151	112	0.1941458	147	0.7909777
8	0.4341235	43	0.3051605	78	0.4392009	113	0.5158154	148	0.2663659
9	0.1883491	44	0.3123417	79	0.1761845	114	0.3228141	149	0.8142152
10	0.5285534	45	1.057107	80	0.4801979	115	0.6823596	150	0.1941458
11	0.1631151	46	0.2052487	81	0.1697756	116	0.8809224	151	1.124193
12	0.2400990	47	0.1823683	82	0.3262303	117	0.5389386	152	0.3329574
13	0.1697756	48	0.6642479	83	0.5993233	118	0.1245812	153	0.1489031
14	0.3015057	49	1.034850	84	0.3796298	119	1.280913	154	0.7504478
15	0.2105807	50	0.9695865	85	0.4077878	120	0.2940600	155	0.2400990
16	0.1489031	51	0.8032488	86	1.086074	121	0.1997744	156	1.492006
17	0.5956123	52	1.081983	87	0.1153398	122	0.6936390	157	0.9069651
18	0.5824375	53	0.4708728	88	0.4755583	123	0.2704958	158	0.4685126
19	0.5071455	54	0.3616843	89	0.6264555	124	0.7094414	159	0.5728415
20	0.1153398	55	0.1631151	90	0.9358413	125	0.2785721	160	0.6659148
21	0.9106247	56	0.7650778	91	0.3395512	126	0.2621709	161	0.1489031
22	0.6011702	57	0.2579077	92	0.7187562	127	0.5491273	162	0.7125599
23	0.4870746	58	0.5409917	93	0.3051605	128	0.2052487	163	0.9603959
24	0.6066772	59	0.1412618	94	0.1245812	129	1.457426	164	0.3796298
25	0.1153398	60	0.4540933	95	1.110302	130	1.011007	165	0.1941458
26	0.6139430	61	0.5862319	96	1.254680	131	1.091166	166	0.4158636
27	0.7977092	62	0.3967645	97	1.123207	132	1.500157	167	0.5650474
28	0.1153398	63	1.579355	98	0.3796298	133	0.4442205	168	0.2902655
29	0.2902655	64	0.5027546	99	0.5179601	134	0.1997744	169	0.2579077
30	0.2745637	65	0.5005447	100	0.9877112	135	0.4565282	170	0.1331829
31	0.2157810	66	0.1561709	101	0.2825237	136	0.1245812	171	0.8996013
32	0.5766991	67	0.2535728	102	0.6758296	137	0.1331829	172	1.298107
33	0.7063093	68	0.2208589	103	0.7094414	138	1.454380	173	0.8809224
34	0.9191071	69	0.2704958	104	0.1883491	139	0.8821800	174	0.5409917
35	0.3939605	70	0.88966880	105	1.113293	140	0.9057420	175	1.530156

DROPLET DATA FOR NEGATIVE 9 (cont'd)

Droplet No.	Diameter (mm)						
176	0.3395512	211	0.5158154	246	0.1412618	281	0.5728415
177	0.5306467	212	1.194013	247	0.2400990	282	0.8682466
178	0.6642479	213	0.1697756	248	0.6369849	283	0.1245812
179	0.4077878	214	0.2052487	249	0.2535728	284	0.4825011
180	0.6404563	215	0.1331829	250	0.2785721	285	0.1412618
181	0.1561709	216	0.1245812	251	0.7650778	286	0.6421849
182	0.1489031	217	0.3707657	252	1.108303	287	0.6139430
183	0.4023139	218	0.1245812	253	0.4392009	288	2.068091
184	0.2940600	219	0.9094065	254	0.8060045	289	0.1331829
185	0.6264555	220	0.9227185	255	0.2258227	290	1.057107
186	0.2354364	221	0.3228141	256	0.2306796	291	0.1245812
187	0.4732214	222	0.4289856	257	0.1153398	292	0.4263935
188	0.3087720	223	0.4417179	258	0.2621709	293	0.4211615
189	0.1331829	224	0.1153398	259	0.2354364	294	1.180943
190	0.2157810	225	0.1331829	260	0.4050601	295	0.1997744
191	0.4916057	226	0.1631151	261	0.4661403	296	0.2354364
192	0.2621709	227	0.1245812	262	0.3123417	297	0.2105807
193	0.1883491	228	2.887337	263	0.4341233	298	1.730097
194	0.2208589	229	0.2535728	264	1.131075	299	0.9298993
195	0.1561709	230	1.345082	265	0.6725409	300	0.6030114
196	0.5591305	231	0.2157810	266	0.2400990	301	0.6121347
197	0.1153398	232	0.1697756	267	0.2535728	302	0.1761845
198	0.1245812	233	0.9843382	268	0.7309912	303	0.1331829
199	0.7141140	234	1.605807	269	0.1245812	304	0.2491625
200	0.7794333	235	2.434463	270	1.399213	305	1.067543
201	0.6984173	236	0.1489031	271	0.1823683	306	0.9854638
202	0.2704958	237	0.2745637	272	0.1823683	307	0.3158711
203	0.1941458	238	0.4023139	273	0.2978061	308	0.1331829
204	0.7822727	239	0.2621709	274	0.1153398	309	1.239568
205	0.7141140	240	1.223364	275	1.281778	310	0.2306796
206	0.3555012	241	1.495716	276	0.3015057	311	0.3492087
207	0.2446727	242	0.1823683	277	0.4613593	312	0.1489031
208	1.408689	243	0.1823683	278	0.2400990	313	0.5389386
209	0.9826631	244	0.8087506	279	0.6856012	314	0.5571443
210	0.96388526	245	1.042321	280	0.4732214	315	0.2902655

DROPLET DATA FOR NEGATIVE 10

Droplet No.	Diameter (mm)								
1	1.206023	36	0.5264518	71	0.4263935	106	0.1153398	141	0.4661403
2	0.9764227	37	0.5709030	72	0.5071455	107	0.7400348	142	0.1561709
3	0.1331829	38	0.2306796	73	0.1489031	108	0.1823683	143	0.2258227
4	0.1331829	39	0.9393883	74	0.6558500	109	1.242242	144	0.3766983
5	0.5937480	40	0.5491273	75	0.3193615	110	1.164875	145	0.2825237
6	0.3051605	41	1.074787	76	0.1245812	111	0.5471048	146	0.3586060
7	0.1883491	42	0.1331829	77	0.3882917	112	1.068581	147	0.2306796
8	0.7202969	43	0.6839823	78	1.052904	113	0.8946584	148	0.3939605
9	0.2978061	44	0.6229062	79	0.8155757	114	0.3087720	149	0.2621709
10	0.2825237	45	0.3296110	80	1.203262	115	0.1941458	150	0.4131892
11	0.8343887	46	0.2354364	81	1.666783	116	0.4104974	151	0.3677634
12	1.474065	47	0.8527870	82	1.376045	117	0.4540933	152	0.1631151
13	0.5071455	48	1.154359	83	0.2052487	118	0.5222232	153	0.5005447
14	0.3428006	49	1.094210	84	0.9287064	119	0.3296110	154	0.6675774
15	0.3123417	50	0.3087720	85	0.3228141	120	0.6807330	155	0.5650474
16	0.7751545	51	0.5200961	86	0.1153398	121	1.601660	156	0.2745637
17	0.6085018	52	0.4565282	87	0.4263935	122	1.374433	157	0.4983250
18	0.2940600	53	0.7233686	88	1.727532	123	0.8462621	158	0.9820831
19	0.7607183	54	1.012103	89	0.7708520	124	0.8958967	159	0.7063093
20	0.5200961	55	0.5306467	90	0.1697756	125	0.3616843	160	0.5368776
21	0.6524605	56	1.093196	91	0.2400990	126	0.6175439	161	0.9499502
22	0.2579077	57	0.2446727	92	0.5611097	127	2.599201	162	0.3523690
23	0.4938556	58	0.4315621	93	0.9718706	128	0.2446727	163	0.1631151
24	0.2052487	59	0.7294731	94	1.055007	129	1.465762	164	0.6299849
25	0.7125599	60	1.226983	95	1.308315	130	0.1153398	165	0.3296110
26	0.3523690	61	1.153398	96	0.5243418	131	0.2621709	166	0.6642479
27	0.5179601	62	0.4263935	97	0.1883491	132	0.9522814	167	0.3939605
28	0.1823683	63	0.1823683	98	0.4417179	133	0.1489031	168	0.5450747
29	0.4685126	64	0.1331829	99	1.127148	134	0.6317422	169	0.3015057
30	0.4442205	65	0.3647365	100	0.1153398	135	1.337644		
31	0.2105807	66	1.449799	101	1.292973	136	0.3087720		
32	0.5306467	67	0.1883491	102	0.4983250	137	0.6121347		
33	0.4960953	68	0.1331829	103	2.009364	138	0.6139430		
34	0.3262303	69	0.3329574	104	1.476320	139	0.2446727		
35	0.7415313	70	1.022998	105	0.2306796	140	0.3123417		

APPENDIX D

DISTRIBUTION LIST

Dr. Frank A. Albini
Northern Forrest Fire Lab
Drawer C
Missoula, MT 59806

Mr. Lou Brown, AMS-120
FAA National Headquarters
800 Independence Avenue, SW.
Washington, DC 20591

Mr. A. Allcock
Department of Industry
Abell House, Room 643
John Islip Street, London
SW14 LM ENGLAND

Mr. Don E. Buse
11B12AB
Phillips Petroleum Company
Bartlesville, OK 74004

Mr. Robert D. Anderson, P.E.
Manager of Engineering
Facet/Quantek, Inc.
P.O. Box 50096
Tulsa, OK 74150

Mr. William A. Callanan
ARCO Chemicals Company
1500 Market Street
Philadelphia, PA 19101

Allied Pilot Association
Equipment Evaluation Comm.
P.O. Box 5524
Arlington, TX 76011

Mr. Ronald Camp
BASF Wyandotte Corporation
1609 Biddle Avenue
Wyandotte, MI 48192

Dr. R. L. Altman
NASA ARC
M.S. 234-1
Moffett Field, CA 94035

Mr. Paul Campbell
244 Green Meadow Way
Palo Alto, CA 94306

Dr. S. J. Armour
Defense Research Establishment
Suffield
Ralston, Alberta
CANADA, T0J 2N0

Mr. Clifford D. Cannon
Transamerica Delaval, Inc.
Wiggins Connectors Division
5000 Triggs Street
Los Angeles, CA 90022

Mr. Robert Armstrong
B-8414 MS-9W61
Boeing Airplane Company
P.O. Box 3707
Seattle, WA 98124

Mr. George A. Cantley
Lear Siegler, Inc.
241 South Abbe Road
P.O. Box 4014
Elyria, OH 44036

Mr. Steven L. Baxter
Conoco, Inc.
Chemicals Research Division
P.O. Box 1267
Ponca City, OK 74601

Captain Ralph Cantrell
University of Bridgeport
U.S. Army ROTC Department
Bridgeport, CT 06601

Dr. D. E. Boswell
Quaker Chemical Corporation
Elm Street
Conshohocken, PA 19428

Dr. Homer W. Carhart
Naval Research Lab
Code 6180
Washington, DC 20375

Mr. Michael Cass
Sundstrand Corporation
4747 Harrison Avenue
Rockford, IL 61101

Mr. B. G. Corman
Exxon Research and Engineering
P.O. Box 4255
Baytown, TX 77520

Dr. Young I. Cho, Ph.D.
Drexel University
College of Engineering
Philadelphia, PA 19104

Mr. Dick Coykendall
United Airlines
San Francisco International
Airport
San Francisco, CA 94128

Mr. Arthur V. Churchill
AFWAL/POSH
Wright Patterson Air Force Base-
Ohio 45433

Mr. Gerald A. Cundiff
General Electric Company
3 Penn Center Plaza
Philadelphia, PA 19102

Mr. J. C. Clerc
Chevron Research Company
P.O. Box 1627
Richmond, CA 94802-0627

Mr. Rick DeMeis
126 Powers Street
Needham, MA 02192

Mr. George A. Coffinberry
General Electric Company
1 Neumann Way
Mail Drop E-186
Cincinnati, OH 45215

Mr. Terence Dixon
Boeing Aerospace Corporation
P.O. Box 3999
M/S 8J-93
Seattle, WA 98124

Mr. Fred W. Cole
Filter Products Division
Facet Enterprises, Inc.
8439 Triad Drive
Greensboro, NC 27409

Mr. Thomas F. Donohue
General Electric Company
1 Neumann Way, Mail Drop H-44
P.O. Box 156301
Cincinnati, OH 45215-6301

Mr. J. Donald Collier
Air Transport Association
of America
1709 New York Avenue, NW
Washington, DC 20006

Mr. William G. Dukek
11 Ridge Road
Summit, NJ 07901

Captain Ralph Combariati
Port Authority of NY and NJ
JFK International Airport
Jamaica, NY 11430

Mr. David W. Eggerding
AMOCO Chemicals Corporation
Research and Development
P.O. Box 400
Naperville, IL 60540

Mr. Edward Conklin
Sikorsky Aircraft
North Main Street
Stratford, CT 06602

Dr. Thor Eklund, ACT-350
DOT/FAA Technical Center
Atlantic City Airport, NJ 08405

Mr. John H. Enders
Flight Safety Foundation
5510 Columbia Pike
Arlington, VA 22204

Dr. Allen E. Fuhs
Department of Aeronautics
Naval Post Graduate School
Monterey, CA 93940

Mr. John T. Eschbaugh
Air Maze Incom International
25000 Miles Road
Cleveland, OH 44198

Dr. Gerald G. Fuller
Chemical Engineering
Stanford University
Stanford, CA 94305

Mr. Anthony Fiorentino
Pratt and Whitney Aircraft
EB2G4
400 Main Street
East Hartford, CT 06108

Y. Funatsu
All Nippon Airways
1-6-6, Tokyo International Airport
Ohta-KU, Tokyo 144
JAPAN

F. Firth
Lucas Aerospace
Vannonstrand Avenue
Englewood, NJ 07632

Henry A. Gill
Lockheed California Company
Building 88, B-6
P.O. Box 551
Burbank, CA 91520

Mr. Kent Fisher
Lockheed California Company
Department 70-30, Building 90
P.O. Box 551
Burbank, CA 91520

Mr. David J. Goldsmith
Eastern Airlines
Miami International Airport
Miami, FL 33148

Mr. David H. Fishman
Technical Planning and Development
United Technologies Inmont
1255 Broad Street
Clifton, NJ 07015

Mr. Stanley Gray
Mechanical Technology Inc.
968 Albany Shaker Road
Latham, NY 12110

Mr. Ray Fitzpatrick
South African Airways
329 Van Riebeeck Road
Glenn Austin Halfway House, 1685
REPUBLIC OF SOUTH AFRICA

Mr. Ray J. Grill
TRW
1766 Sunset Drive
Richmond Heights, OH 44124

Dr. Kendall Foley
Hercules Inc.
Research Center
Wilmington, DE 19899

G. Haigh
Air Canada
Air Canada Base, Montreal
International Airport
Quebec, CANADA H4Y 1 C2

Mr. Robert Friedman
NASA Lewis Research Center
M/S 6-9
21000 Brookpark Road
Cleveland, OH 44135

Lit S. Han
Ohio State University
206 W. 18th Avenue
Columbus, OH 43210

N. Hardy
United Airlines
SFOEG, MOC
San Francisco International Airport
California 94128

Cyrus P. Henry
E. I. Dupont De Nemours
and Company
Petroleum Lab
Wilmington, DE 19898

R. Hileman
Texaco, Inc.
Box 509
Beacon, NY 12508

W. Hock
Grumman Aerospace Corporation
B 14 035
111 Stewart Avenue
Bethpage, NJ 11714

Arthur Hoffman
American Cynamid
1937 West Main Street
Stamford, CT 06904

LCDR William Holland
Department of the Navy
NAIR 518
Naval Air Systems Command
Washington, DC 20361

Robert L. Hoover
Box 10850 Cave Creek Stage
Phoenix, AZ 85020

Mr. Thomas G. Moreff
Federal Aviation Administration
AEU-101
c/o American Embassy
APO New York 09667-1011

Mr. Gary L. Horton
Chemical Research Division
Conoco, Inc.
P.O. Box 1267
Ponca City, OK 74603

Major Hudson
Air Force Inspection and Safety
SEDM
Norton Air Force Base, CA 92499

Mr. Stephen L. Imbrogno
Pratt and Whitney Aircraft Group
Government Products Division
M/S 711-52
West Palm Beach, FL 33402

Dr. Wolfgang Immel
BASF Aktiengesellschaft
Technologie und Produktionsplanung
6700 Ludwigshafen
WEST GERMANY

M. C. Ingham
Chevron Research Company
P.O. Box 1627
Richmond, CA 94802-0627

G. Jahrstorfer
Chandler Evans, Inc.
Charter Oak Boulevard
West Hartford, CT 06110-0651

Mr. J. P. Jamieson
National Gas Turbine Establishment
Pyestock, Farnborough
Hants GU14 OLS
ENGLAND

Mr. Eric Jevons
Chandler Evans, Inc.
Charter Oak Boulevard
Box 10651
West Hartford, CT 06110-0651

Mr. Stanley Jones
Pan American World Airways
JFK International Airport
New York, NY 11420

R. Kassinger
Exxon International Company
Commercial Department
200 Park Avenue
Florham, NJ 07932

Dr. C. W. Kauffman
The University of Michigan
Gas Dynamics Laboratories
Aerospace Engineering Building
Ann Arbor, MI 48109

Mr. Perry Kirklin
Mobil Research and Development
Corporation
Billingsport Road
Paulsboro, NJ 08066

Mr. R. Kirsch, AWS-120
FAA National Headquarters
800 Independence Avenue, SW.
Washington, DC 20591

Mr. John Kirzovensky
Naval Air Propulsion Center
Code PE71
1440 Parkway Avenue
Trenton, NJ 08628

Mr. W. Peter Kochis
FAA Safety Programs
Division, ASF-300
800 Independence Avenue, SW.
Washington, DC 20591

Mr. Rob Koller
Rohm and Haas
727 Norristown Road
Spring House, PA 19477

Mr. Robert J. Kostelnik
ARCO Chemical Company
3801 West Chester Pike
Newtown Square, PA 19073

Mr. J. I. Knepper
Petrolite Corporation
369 Marshall Avenue
St. Louis, MO 63119

Dr. John Krynetsky
Fuels and Petroleum Products
4904 Cumberland Avenue
Chevy Chase, MD 20015

Dr. Karl Laden
Carter-Wallace, Inc.
Half Acre Road
Cranbury, NJ 08512

Mr. Thomas P. Lally, Jr.
Senior Marketing Specialist
Aircraft Porous Media, Inc.
Pinellas Park, FL 33565

Dr. R. Landel
Jet Propulsion Lab
4800 Oak Grove Drive
Pasadena, CA 91103

R. Laurens
Rolls-Royce, Inc.
1895 Phoenix Boulevard
Atlanta, GA 30349

Mr. Richard J. Linn
American Airlines
MD 4H14
P.O. Box 61616
Dallas/Fort Worth Airport, TX 75261

P. Longjohn
Clagon Corporation
P.O. Box 1346
Pittsburgh, PA 15230

Mr. Richard R. Lyman
Lear Siegler, Inc.
Energy Products Division
2040 East Dyer Road
Santa Ana, CA 92702

Dr. Richard Mannheimer
Southwest Research Institute
8500 Culebra Road
San Antonio, TX 78284

Captain A. S. Mattox, Jr.
Allied Pilots Association
12723 Brewster Circle
Woodbridge, VA 22191

Mr. James McAbee
ICI Americas, Inc.
Specialty Chemicals Division
Wilmington, DE 19897

Mr. Charles McGuire
Department of Transportation
400 7th Street, SW. (P-5)
Washington, DC 20590

M. L. McMillan
G.M. Research
Fuels and Lubricants Department
Warren, MI 48090

Mr. Peter Meiklem
British Embassy
3100 Massachusetts Avenue, NW
Washington, DC 20008

Mr. G. Chris Meldrum
Texaco Company
P.O. Box 430
Bellaire, TX 77401

Dr. Robert E. Miller
c/o Dr. S. P. Wilford
Royal Aircraft Establishment
Farnborough, Hants
GU146TD, ENGLAND

Mr. Robert J. Moore
Shell Chemical Company
Box 2463
Houston, TX 77001

Mr. Peter D. Moss
American Hoechst Corporation
Route 206 North
Somerville, NJ 08876

Mr. David Nesterok, ACT-2P
DOT/FAA Technical Center
Atlantic City Airport, NJ 08405

Mr. Warren D. Niederhauser
Rohm and Haas Company
727 Norristown Road
Spring House, PA 19477

J. J. O'Donnell
Airline Pilots Association
1625 Massachusetts Avenue, NW.
Washington, DC 20036

Dean Oliva
Lockheed
Department 7475/Building 229A
P.O. Box 551, Plant 2
Burbank, CA 91520

Dr. Robert C. Oliver
Institute for Defense Analyses
1801 North Bauregard Street
Alexandria, VA 22311

Mr. James H. O'Mara
Rohm and Haas
727 Norristown Road
Spring House, PA 19477

Mr. George Opdyke
AVCO Lycoming Division
550 South Main Street
Stratford, CT 06497

Dr. Robert H. Page
Texas A&M University
College of Engineering
College Station, TX 77884

Chris Papastrat
CEE Electronics, Inc.
8875 Midnight Pass Road
Sarasota, FL 33581

Mr. Roy E. Pardue
Lockheed/Georgia Company
86 South Cubb Drive
Marietta, GA 30063

Mr. Sam Paton
El Paso Products
P.O. Box 3986
Odessa, TX 79760

Mr. Tom Peacock
Douglas Aircraft Company
3855 Lakewood Boulevard
Longbeach, CA 90846

R. D. Pharby
Petro Canada
Sheridan Park
Mississauga, Ontario
CANADA, L5K1A8

Mr. John Pullekins
Air Products and Chemicals
Industrial Chemical Division
P.O. Box 538
Allentown, PA 18105

Dr. Andy Powell
Saudia - CC 836
P.O. Box #167
Jeddah
SAUDI ARABIA

Mr. Horst Rademacher
68 Myrtle Street
Boston, MA 02114

Mr. William Radenbaugh
General Electric Company
Manager, Operational Planning
1000 Western Avenue
Lynn, MA 01910

C. C. Randall, P.E.
Lockheed Georgia Company
072-47 Zone 418
Marietta, GA 30063

Mr. Richard W. Reiter
National Starch and Chemical
Box 6500
10 Finderne Avenue
Bridgewater, NJ 08807

M. Rippen
Pratt and Whitney Aircraft
Government Products Division
P.O. Box 2691
West Palm Beach, FL 33402

Mr. Charles Rivers
ICI Americas, Inc.
Wilmington, DE 19897

Mr. Russell Rogers
Aeroquip Corporation
Corporate Engineering
Jackson, MI 49203

J. Romans
Hughes Association, Inc.
9111 Louis Avenue
Silver Spring, MD 20910

E. T. Rockey
Northrop Corporation
Aircraft Division
One Northrop Avenue
Hawthorne, CA 90250

Dr. V. Sarohia
Jet Propulsion Lab
M/S 125-214
4800 Oak Grove Drive
Pasadena, CA 91109

Mr. George Savins
Mobil Oil Research and
Development
P.O. Box 819047
Dallas, TX 75381

Dr. Barry Scallet
Anheuser-Busch Corporation
Central Research Inc.
P.O. Box 11841
Clayton, MO 63105

Mr. Forrest W. Schaeke
U.S. Army MERADCOM
Fort Belvoir, VA 22060-5606

Mr. Barry Scott, ADL-31
P.O. Box 25
NASA Ames Research Center
Moffett Field, CA 94035

Professor Valentinas Sernas
Rutgers University
College of Engineering
P.O. Box 909
Piscataway, NJ 08854

Mr. Subhash Shah
Allied Chemical
Syracuse Research Lab
P.O. Box 6
Salisbury, NY 13209

Dr. Hakam Singh, Ph.D.
Product Chemical and Research
Corporation
2920 Empire Avenue
Burbank, CA 91504

Ms. Dana Smith
ARCO Chemical Company
1500 Market Street
32nd Floor
Philadelphia, PA 19101

Mr. H. Daniel Smith
Manager, Research and Development
Engineered Fabrics Division
Goodyear Aerospace Corporation
Akron, OH 44315

S. Sokolsky
Aerospace Corporation
P.O. Box 91957
Los Angeles, CA 90009

Mr. Leo Stamler
Gull Airborne Instruments, Inc.
395 Oser Avenue
Smithtowne, NY

Mr. Barry Stewart
Olin Chemicals
Brandenburg, KY 40108

Dr. Warren C. Strahle
Georgia Institute of Technology
School of Aerospace Engineering
Atlanta, GA 30332

Mr. Peter A. Stranges
1420 16th Street, NW.
Washington, DC 20006

Mr. Kurt H. Strauss
Consultant, Aviation Fuels
116 Hooker Avenue
Poughkeepsie, NY 12601

Mr. Dick Stutz
Sikorsky Aircraft
Engineering Department
Stratford, CT 06602

Mr. A. F. Taylor
Cranfield Institute of Technology
Cranfield, Bedford, MK 43 0AL
ENGLAND

Dr. W. F. Taylor
Exxon Research and Engineering Company
Products Research Division
P.O. Box 51
Linden, NJ 07036

Dr. James Teng, Ph.D.
Anheuser-Busch Corporation
1101 Wyoming Street
St. Louis, MO 63118

Mr. Joseph Thibodeau
Goodyear Aerospace Corporation
1210 Massillon Road
Akron, OH 44315

Mr. Richard G. Thrush
Lear Siegler, Inc.
241 South Abbe Road
P.O. Box 4014
Elyria, OH 44036

Mr. Dick Tobiason
Air Transport Association
1709 New York Avenue, NW.
Washington, DC 20006

Dr. F. F. Tolle
Boeing Military Airplane Company
P.O. Box 3707
M/S 4152
Seattle, WA 98124

Mr. R. Hugh Trask
Southland Corporation
849 Coast Boulevard
LaJolla, CA 92034

M. Trimble
Delta Airlines
DEAT 568
Atlanta International Airport
Atlanta, GA 30320

Mr. T. Ted Tsue
Boeing Aerospace Company
P.O. Box 3999
M/S 45-07
Seattle, WA 98124

Trans World Airlines, Inc.
Kansas City International Airport
2-280
P.O. Box 20126
Kansas City, MO 64195

Mr. Robert Umschied
M.S.E.-6
9709 East Central
Wichita, KS 19328

Mr. Ed Versaw
Lockheed/California Company
P.O. Box 551
Burbank, CA 91520

J. F. Vitkuske
Dow Chemical Company
1702 Building
Midland, MI 48640

Mr. Fred Waite
Imperial Chemical Industries PLC
Paints Division
Mexham Road, Slough SL2 5DS
ENGLAND

Dr. G. J. Walter
Sherwin-Williams Company
501 Murray Road
Cincinnati, OH 45217

H. Weinberg
Exxon Research and
Engineering Company
P.O. Box 45
Linden, NJ 07036

Mr. Paul Weitz
Simmonds Precision Instruments
Panton Road
Vergennes, VT 05491

Mr. John White
National Transportation
Safety Board
800 Independence Avenue, SW.
Washington, DC 20594

Mr. Richard White
Denry White, Inc.
P.O. Box 30088
Cleveland, OH 44130

Dr. S. P. Wilford
Royal Aircraft Establishment
Farnborough, Hants
GU146TD
ENGLAND

R. P. Williams
Phillips Petroleum
107 Catalyst Lab
Bartlesville, OK 74004

R. E. Zalesky
Lockheed California Company
P.O. Box 551
Burbank, CA 91520

Civil Aviation Authority (5)
Aviation House
129 Kingsway
London WC2B 6NN England

DOT-FAA AEU-500 (5)
American Embassy
APO New York, NY 09667

Embassy of Australia (1)
Civil Air Attaché
1601 Mass. Ave. NW
Washington, DC 20036

University of California (1)
Service Dept Institute of
Transportation Standard Lib
412 McLaughlin Hall
Berkeley, CA 94720

Scientific & Tech. Info FAC (1)
ATTN: NASA Rep.
P.O. Box 8757 BWI Airport
Baltimore, MD 21240

British Embassy (1)
Civil Air Attaché ATS
3100 Mass Ave. NW
Washington, DC 20008

Northwestern University (1)
Trisnet Repository
Transportation Center Library
Evanston, ILL 60201

Director DuCentre Exp DE LA (1)
Navigation Aerineene
9141 Orly, France

ANE-40	(2)	ACT-624	(2)	ASW-53B	(2)
ASW-52C4	(2)	AAL-62	(2)	AAC-44.4	(2)
APM-13 Nigro	(2)	M-493.2 Bldg. 10A	(5)	ACE-66	(2)
AEA-66.1	(3)	APM-1	(1)	ADL-1	(1)
ADL-32 North	(1)	APA-300	(1)	ALG-300	(1)
AES-3	(1)	AGL-60	(2)	ACT-8	(1)
ANM-60	(2)				

FAA, Chief, Civil Aviation
Madrid, Spain
c/o American Embassy
APO-New York 09285-0001

Al Astorga (1)
Federal Aviation
Administration (CAAG)
American Embassy, Box 38
APO-New York 09285-0001

Dick Tobiason (1)
ATA of America
1709 New York Avenue, NW
Washington, DC 20006

Burton Chesterfield, DMA-603 (1)
DOT Transportation Safety Inst.
6500 South McArthur Blvd.
Oklahoma City, OK 73125

FAA Anchorage ACO
701 C Street, Box 14
Anchorage, Alaska 99513

FAA Fort Worth ACO
P.O. Box 1689
Fort Worth, TX 76101

FAA Atlanta ACO
1075 Inner Loop Road
College Park, Georgia 30337

FAA Long Beach ACO
4344 Donald Douglas Drive
Long Beach, CA 90808

FAA Boston ACO
12 New England Executive Park
Burlington, Mass. 01803

FAA Los Angeles ACO
P.O. Box 92007, Worldway Postal Center
Hawthorne, CA 90009

FAA Brussels ACO
% American Embassy, APO,
New York, NY 09667

FAA New York ACO
181 So. Franklin Ave., Room 202
Valley Stream, NY 11581

FAA Chicago ACO
2300 E. Devon, Room.232
Des Plains, Illinois 6008

FAA Seattle ACO
17900 Pacific Highway South, C-68966
Seattle, Washington 98168

FAA Denver
10455 East 25th Ave., Suite 307
Aurora, Colorado 80016

FAA Wichita ACO
Mid Continent Airport, Room 100 FAA Bldg.
1891 Airport Road
Wichita, KA 67209

Frank Taylor
3542 Church Road
Ellicott City, MD 21043